Review: Elaboration, structure, and mechanical properties of oxynitride glasses

Alexis Duval, Patrick Houizot, Tanguy Rouxel

Review: Elaboration, structure and mechanical properties of oxynitride glasses

Alexis Duval[a], Patrick Houizot[a] and Tanguy Rouxel[a,b*]

[a]Glass Mechanics Lab., Physics Institute, IPR UMR 6251, University of Rennes 1, Campus de Beaulieu, 35042 Rennes cedex, France.

[b]Institut Universitaire de France.

*corresponding author: tanguy.rouxel@univ-rennes1.fr

ABSTRACT

Oxynitride glasses are glasses where three-fold coordinated nitrogen atoms substitute for 2-fold oxygen ones, hence resulting in a larger interatomic cross-linking degree. Such glasses were first observed at the grain boundary in silicon nitride ceramics, where they govern the high temperature behavior. Later, they were prepared as bulk materials and motivated numerous researches thanks to their large viscosity, glass transition range, elastic moduli, hardness and fracture toughness among inorganic and non-metallic glasses. The different chemical systems that were investigated, the synthesis routes and the sources for these exceptional mechanical properties are reviewed. Oxynitride glasses are not easy to process and suffer from the loss of transparency as nitrogen is incorporated over some critical content. Nevertheless, they are attractive "specialty" glasses in various niche areas thanks to their large refractive index and dielectric constant, improved chemical durability, high softening point, … and in the first place to their exceptional mechanical properties.

1. INTRODUCTION

Nitrogen is a common element in the universe with the $1s^2\ 2s^2\ 2p^3$ electron configuration. It is found in gases like N_2 or NH_3, in organic compounds where it forms a wide variety of bonds

and functional groups with various elements, as well as in ceramics. In the case of silicon nitride (Si_3N_4), nitrogen is three-fold coordinated to silicon (sp^2 hybridization). This results in an increase of the cross-linking degree in comparison with oxygen, which is two-fold coordinated (like in SiO_2). Besides, metal-nitrogen bonds are more covalent than metal-oxygen bonds because of the lower electronegativity of nitrogen (χ_N = 3.04 and χ_O = 3.44). Nitride ceramics, and especially those based on silicon nitride (such as the "sialons"), are advantaged by excellent mechanical properties (hardness, stiffness, toughness and strength) at room temperature, and remain strong ($\sigma_r \approx 1$ GPa) and creep-resistant up to 1300 °C in air [1]. Nitrides may also exhibit interesting functional properties such as thermal and electrical conductivities (AlN) and semiconductivity (GaN) [2].

In the 1960' Mulfinger [3] [4] introduced a low amount of nitrogen in oxide melts by using various gases, such as ammonia. In the 1970' oxynitride glasses were discovered at grain-boundaries in silicon nitride ceramics by K. H. Jack, when compounds such as Y_2O_3 were used as sintering additives for Si_3N_4 [1] [4]. In order to better understand the role of this secondary intergranular phase on the mechanical properties of silicon nitride ceramics, and in particular on their creep behavior, oxynitride glasses were synthesized as bulk materials, by adding silicon nitride as a nitrogen source in oxide powder mixtures. Worldwide investigations (Fig. 1) on oxynitride glasses from various chemical systems (silicon-based, phosphate-based, etc) revealed remarkable mechanical properties, both at room and at elevated temperature, with fracture toughness being typically twice larger for nitrogen glasses than for the parent oxide composition, and a viscosity coefficient increasing by about three orders of magnitude as one out of five oxygen atom is substituted by a nitrogen one. About 15 papers in international scientific journals have been published yearly since 1980. Nevertheless, the loss of transparency at nitrogen contents larger than 15 eq. % led to broaden the scope of applications beyond optics. Emerging fields include hardening and functionalization of surfaces by means of amorphous

oxynitride thin film deposition, and biocompatible and bioactive materials for implantology. Besides, present investigations focus on improving the atmosphere control and the purity of the starting powders, and explore new synthesis routes to achieve a better transparency at large nitrogen content.

2. GLASS CHEMICAL SYSTEMS

2.1 Silicate-based

Several oxynitride glasses systems were explored over the past decades [4], among which silicate-based oxynitride glasses were probably the most studied. Cations were usually added to reduce the melting temperatures of the starting mixtures, which would otherwise require melting temperatures high enough to cause the decomposition of the melt (formation of Si and N_2 from Si_3N_4) [5], and to ease the glass formation, resulting in M-Si-O-N systems where M can be a combination of secondary cations and represents alkalines [6], alkaline-earths [7 8 9 10 11], or rare-earths (*RE*) [12 13 14]. The addition of aluminum to form M-Si-Al-O-N glasses was also often reported [15 16 17 18 19 20 21 22]. Aluminum was found to increase nitrogen solubility, to widen the range of glass formation (Fig. 2), and to prevent demixing. Y-Si-Al-O-N glasses were found very successful in this regard [23 24 25]. Other sub-system includes M-Si-Mg-O-N glasses, as Mg also widen the compositional range, while resulting in close mechanical properties [26 27 28 29 30]. The nitrogen content of oxynitride glasses is usually expressed either in at %, wt % or eq % (equivalent percent). The eq. % in nitrogen (also noted e/o) is expressed as: eq. % $N = \frac{3N*100}{3N+2O}$, where N and O are the molar concentrations of nitrogen and oxygen respectively. It is calculated separately for anions and cations, and accounts both for the chemical composition and for the valence of the ions. In the presence of aluminum and/or magnesium, homogeneous glass batches, few cm^3 large, with up to 30 e/o N can be obtained [31 32], while transparency is retained for nitrogen contents below 15 e/o N (Fig. 3).

Mixed glasses families were explored, as in the M-Si-P-O-N system [33] [34] [35] [36], of which the Na-Ca-Si-P-O-N (with nitrogen content up to 28.5 e/o) was investigated recently because of its interesting bioactive properties, that could be interesting for medical use. Indeed, a major issue with bioactive glasses is their low compressive strength, and oxynitride glasses are promising in this regard.

Few glasses in the M-Si-B-O-N system were reported, because the melts experienced large weight losses in boron as it is prone to volatilization at high temperatures [37] [38]. However, the sol-gel route in a Na-Ba-Si-B-Al-O-N glass led to more satisfying glasses with higher nitrogen content, up to a few wt.% (about 6 e/o [39] [40]). They present an increase in Young's modulus (*E*) with increasing nitrogen, as in silicate-based oxynitride glasses.

2.2 Phosphate-based

M-P-O-N glasses are usually synthesized either via the ammonolysis route for large batches (to be discussed later on) [41] [42] [43] [44] [45] [46] [47] or via sputtering for thin films [48], with nitrogen content up to 33.5 e/o or even slightly higher, although it is unsure if glasses richer in nitrogen are of the same nature [46] [49]. They are promising materials as solid-state electrolytes due to their strong ionic conductivity and chemical durability, especially the Li-P-O-N system [50] [51] [52]. Moreover, their tendency to devitrify is smaller than for their oxide counterparts, they are less hygroscopic and exhibit larger elastic moduli [49] [53].

2.3 Borate-based

M-B-O-N oxynitride glasses were not studied much. Amorphous thin films were obtained in the Li-B-O-N system by magnetron sputtering under nitrogen [54] [55]. In this latter system, the formation of B-N-B bonds was found to enhance the diffusion of Li ions, likely via some charge delocalization (within these bonds) and thus thanks to the reduction of the electrostatic

interaction with the Li ions. Besides, the nature of the B-N bonds was found to depend on the composition of the sputtering target.

The solubility of nitrogen in borate-based glasses is quite low no matter the synthesis route, being only a few tenths of wt% (about 1 e/o) [56] [57] [58] [59] [60]. On a side note, one paper claimed to have synthesized an oxynitride glass free from Si, P and B in the Ca-Ba-Mg-Al-O-N system, showing a similar increase in T_g and a decrease of the thermal expansion coefficient with increasing nitrogen content as in other oxynitride glasses, but no further report dealt with this system since then [61].

3 SYNTHESIS

3.1 Synthesis routes

a) Melting

The first synthesis route consists in melting the various oxides (SiO_2, Al_2O_3, MgO, Y_2O_3, etc.) and nitrides (mostly Si_3N_4 and AlN) precursors at temperatures ranging from 1300 to 1850 °C depending on the melt composition [62] [63] [64], so that every reactant is melted and that the mixture viscosity is low enough to quench it. This step usually lasts for an hour in order to obtain a homogeneous melt. The nitrides may be mixed with the already synthesized oxide glass to prevent compounds decomposition due to side reactions, which will be further detailed in § 3.5 a) [5]. Both melting and annealing stages must be conducted in oxygen free environment to limit the loss of substituted nitrogen atoms in the liquid. Nitrogen atmosphere has been mostly used so far, although argon or argon-N_2 or argon-H_2 mixtures were sometimes used [65], mostly in gas flow protecting devices (Fig. 4). In addition, large cooling rates (typically from 600 to 1000 °C.min^{-1}) are required as soon as the liquid composition lies close to the border of the glass forming region [66]. Glasses cooled with slow cooling rates turn out to be more transparent [10] [62].

Other reactants were sometimes used, such as fluorides in the case of oxyfluoronitride glasses [67] or hydroxides [58]. More recently, hydrides and metals were used as some are highly reacting with nitrogen when heated, and form glasses with much larger nitrogen content compared to those obtained by conventional melting (up to 68 e/o [12 68]). However, some metals can reduce several oxides like silica in the melts, leading to formation of metallic micro-particles including silicides [12 68 69]. Alternatively, oxynitride glasses were prepared with nitrogen overpressures up to 200 MPa successfully preventing nitrogen loss in the glass [65 70], or by self-propagating high-temperature combustion synthesis (*SHS*) [57].

b) Ammonolysis of melts

A second way to synthesize oxynitride glasses consists in realizing the ammonolysis of the glass melt *i.e.* the substitution of oxygen for nitrogen using N_2 and/or NH_3 flowing gas, at temperatures typically below 900 °C in the case of phosphate-based glasses [41 71]. For example, starting from a $NaPO_3$ glass, the reaction is:

$$NaPO_3 + \frac{2x}{3} NH_3 \longrightarrow NaPO_{3-x}N_{2x/3} + x\ H_2O \quad (1)$$

This reaction must take place at temperatures larger than 600 °C to allow for the decomposition of NH_3 but smaller than 800 °C to prevent from the reduction of phosphorous and the formation of a colored and heterogeneous glass. The benefit of this synthesis route is to add nitrogen to the medium but without its counterion, in opposition to the use of nitrides. Furthermore, it is more suitable to oxides such as P_2O_5 that suffer from volatilization at high temperatures, or because of their reactivity with nitrides [72], and is mostly used for phosphate-based oxynitrides [5]. However, these exotic synthesis routes take longer time (>10 h) in order to incorporate large amounts of nitrogen, due to the slower liquid/gas reaction kinetics [3 73]. The resulting glasses

usually are transparent, and it should be noted that the nitrogen content increases with increasing temperature [41 42 53 74 75 76]. Nevertheless, glasses turn black if the ammonolysis temperature is too high because of a reduction reaction of the phosphorus oxides [71 73 77].

c) Sol-gel

The third way is the sol-gel route, which consists firstly to synthesize a gel using reactants like alkoxides. Less common precursors composed of Si-CH_3 and/or Si-H groups may be used, as they are highly reactive to NH_3 [78 79]. The second step consists to realise the gel (or else the colloidal silica [80]) ammonolysis according to various mechanisms such as reactions (2) to (4) [39 79 81 82]. This step is carried out using an ammonia flow at temperatures ranging from 400 to 1300 °C for a few hours, the purpose of the gas flow being to remove the gaseous products formed (alcohols and water), therefore displacing the equilibrium and allowing more nitrogen to be substituted. In the case of a silica gel:

$$\equiv Si{-}OH + NH_3 \longrightarrow \equiv Si{-}NH_2 + H_2O \xrightarrow{\equiv Si{-}OH,\ NH_3} \equiv Si{-}N(H)(Si\equiv) \xrightarrow{\equiv Si{-}OH,\ NH_3} \equiv Si{-}N(Si\equiv)_2 \quad (2)$$

$$\equiv Si{-}O{-}Si\equiv + NH_3 \longrightarrow \equiv Si{-}NH_2 + HO{-}Si\equiv \quad (3)$$

$$\equiv Si{-}OR + NH_3 \longrightarrow \equiv Si{-}NH_2 + ROH \quad (4)$$

This synthesis route also presents the benefit to avoid the use nitrides, thus broadening the range of glass compositions. The glasses were described as optically transparent, in opposition to glasses obtained using the melting route with sometimes high nitrogen content (close to 38 e/o [82] or even higher in the case of oxynitride glasses fibres [83]).

An analogous route uses polymers like polysiloxanes which, once pyrolyzed under ammonia, give oxynitride glasses [84 85]. The pyrolysis temperature and atmosphere are crucial, especially

to prevent trapped free-carbon within the structure, of which a content even lower than 0.2 wt.% may colour the glass.

3.2 Starting materials

Various compounds, for instance SiO_2, exhibit a few amounts of adsorbed water even at temperatures as high as 1000 °C when the particles size is very fine [86]. It can decompose nitrides during the synthesis according to [87]:

$$Si_3N_{4(s)} + 3\ H_2O_{(g)} \xrightarrow{\Delta} 3\ SiO_{(g)} + 2\ N_{2(g)} + 3\ H_{2(g)} \quad (5)$$

Some oxides such as Li_2O are brought in the medium starting from carbonated precursors, because of their reactivity with the ambient atmosphere. It is thus important to realize their complete decarbonization to both free the melt from CO_2 bubbles and to prevent the oxidation of Si_3N_4 (and thus the loss of nitrogen in the glass) via various mechanisms [87 88]. In the case of Li_2CO_3:

$$Li_2CO_{3(s)} \xrightarrow{\Delta} Li_2O_{(s)} + CO_{2(g)} \quad (6)$$

$$Si_3N_{4(s)} + 6\ CO_{2(g)} \xrightarrow{\Delta} 3\ SiO_{2(s)} + 6\ CO_{(g)} + 2\ N_{2(g)} \quad (7)$$

Impurities are other sources of side reactions and have to be considered even in weak quantities, especially iron (as metal or oxides), a common impurity in reactants used in oxynitride glasses synthesis [89]. In the presence of Si_3N_4, the various iron containing impurity species may result in metallic micro/nano inclusions (such as iron silicides), even at temperatures as low as 1200 °C:

$$Si_3N_{4(s)} + 6\ FeO_{(s)} \xrightarrow{\Delta} 3\ SiO_{2(s)} + 6\ Fe_{(s)} + 2\ N_{2(g)} \quad (8)$$

$$Si_3N_{4(s)} + FeO_{(s)} \xrightarrow{\Delta} SiO_{(g)} + FeSi_2 + 2\ N_{2(g)} \quad (9)$$

$$Si_3N_{4(s)} + Fe_{(s)} \xrightarrow{\Delta} FeSi_3 + 2\ N_{2(g)} \quad (10)$$

Consequently the glass becomes opaque, even for a content of inclusions as small as 0.05 vol.% [62 90 91].

In the case of phosphorous oxynitride glasses, which were first reported in the early 80s by Marchand [71], phosphate salts such as $NaPO_3$ and $LiPO_3$ [34 42 92 47 93 94 71], ammonium phosphates [53 95], phosphoric acid [45] as well as phosphate oxide glasses are used as starting materials. Under NH_3 flowing gas, the 3-fold coordinated N^{3-} anions may subsequently result in the following oxidation reaction,

$$N^{3-} \longrightarrow \frac{1}{2} N_2\nearrow + 3\, e^- \quad (11)$$

which confers a reducing character to the oxynitride liquid that may promote the reduction of cations such as copper or silver to metals.

3.3 Crucibles

The materials for the crucibles in which the glasses are synthesized is of paramount importance, as it may interact in various ways with the melt. Some should be avoided, such as platinum crucibles as they form alloys with the reactants under reducing atmospheres [26 96], oxide-based crucibles dissolve in the melt, zirconium and tantalum crucibles are oxidized because of the reactants [5], and graphite crucibles might pollute the melt or even reduce oxides such as P_2O_5 [97 98]. Graphite crucibles coated with boron nitride or pure BN crucibles allow to maintain a reducing atmosphere (local scale) and facilitate the demoulding of the glasses [63]. However, the use of BN results in the presence of BN inclusions in the glasses [16 26 63]. Crucibles made in transition metals such as Mo, W and Nb were mostly not found to react with the powder mixtures or with the nitrided melt, but the dissolution of Nb and the formation of molybdenum silicides were sometimes observed [8 34 88 99]. Sometimes, the crucibles are covered so that the

gaseous SiO molecules produced by various reactions are trapped inside, thus maintaining a partial pressure in SiO large enough to prevent further decomposition of the compounds (see § 3.5) [100 101].

3.4 Atmosphere

In comparison with N_2, NH_3 is more favorable to the nitridation process, both in terms of quantity and kinetics [73 102]. However, the processing of oxynitride glasses under NH_3 flowing gas is limited to temperatures below 800 °C due to the loss of reactivity of NH_3 at higher temperature, which follows the decomposition of NH_3 into N_2 and H_2 gas. So far, the synthesis under ammonia chiefly concerned phosphate-based oxynitride compositions. As soon as temperatures higher than 1300 °C are required, as in the case of silicon oxynitrides, argon or N_2 gas atmosphere are used and nitrogen is further incorporated to the powder mixture by means of nitrided compounds (Si_3N_4, AlN). In this later case it is mandatory to keep the oxygen partial pressure as small as possible. Although argon gas can be used, a large partial pressure of N_2 helps preventing side reactions.

3.5 Choice of the chemical composition

The choice of the oxynitride glasses chemical composition depends much on the stability of the reactants in the melt considering the synthesis atmosphere. In fact, several side reactions may alter the chemical composition of the glass and thus its properties, in addition to heterogeneities like trapped gas bubbles due to the high viscosity of oxynitride glass melts, or metallic micro-particles (as discussed before).

a) Side reactions

In the case of silicate glasses, several possible side reactions were reported [5 26 103 104 105 106]:

$$Si_3N_{4(s)} + 3\ O_{2(g)} \xrightarrow{\Delta} 3\ SiO_{2(l)} + 2\ N_{2(g)} \quad (12)$$

$$Si_3N_{4(s)} + \frac{3}{2}\ O_{2(g)} \xrightarrow{\Delta} 3\ SiO_{(g)} + 2\ N_{2(g)} \quad (13)$$

$$Si_3N_{4(s)} \xrightarrow{\Delta} 3\ Si_{(l)} + 2\ N_{2(g)} \quad (14)$$

$$SiO_{2(l)} \xrightarrow{\Delta} SiO_{(g)} + \frac{1}{2}\ O_{2(g)} \quad (15)$$

$$Si_3N_{4(s)} + SiO_{2(s)} \xrightarrow{\Delta} 2\ SiO_{(g)} + 2\ Si_{(l)} + 2\ N_{2(g)} \quad (16)$$

$$Si_3N_{4(s)} + 3\ SiO_{2(s)} \xrightarrow{\Delta} 6\ SiO_{(g)} + 2\ N_{2(g)} \quad (17)$$

$$Si_3N_{4(s)} + Al_2O_{3(s)} \xrightarrow{\Delta} 3\ SiO_{(g)} + 2\ AlN_{(s)} + N_{2(g)} \quad (18)$$

Reactions (12), (13), (14) and (17) can be prevented by maintaining a large enough partial pressure in N_2, but this will not be sufficient if the temperature is too high [26] [103] [104]. However, it was shown based on a thermodynamic analysis that as soon as the temperature is high enough, the decomposition reactions (16) and (18) cannot be suppressed, even if a large partial pressure in N_2 is maintained [103]. Therefore, reactions (15) (16) and (18) can only be avoided by lowering the synthesis temperature [105]. The addition of metallic silicon to the melt effectively limits the formation of bubbles in the glass according to reactions (14) and (16), but metallic silicon or silicide domains remain in the glass [107].

The use of Ellingham diagrams quickly tells whether the reduction of an oxide by a nitride is thermodynamically favorable ($\Delta G < 0$). For example, the reduction of oxides such as Li_2O, Al_2O_3, MgO, CaO and BaO by Si_3N_4 is not thermodynamically feasible in the usual temperature range of syntheses, in opposition to Na_2O P_2O_5 K_2O Cs_2O and ZnO [5] [88] [72] [108] [109]. Nevertheless, this reduction is sometimes observed via an exothermic reaction in the form of vapours [37]. However, let us recall that such a tool brings no information about the kinetics. In the case of P_2O_5, the reduction reaction is written:

$$Si_3N_{4(s)} + \frac{6}{5}\ P_2O_{5(s)} \xrightarrow{\Delta} 3\ SiO_{2(s)} + \frac{6}{5}\ P_{2(g)} + 2\ N_{2(g)} \quad (19)$$

Note that weight losses in P in the M-Si-P-O-N system can partly be avoided using a 3-step synthesis [36]: The oxide-based glass is first synthesized, then the N-containing glass is obtained via the melting route by crushing beforehand the previous glass with Si_3N_4, and finally the N-P-containing glass is synthesized in the same way by crushing beforehand the N-containing glass with P_2O_5.

Since reactions (5) to (10) and (12) to (19) are thermally activated, the lowest synthesis temperature needed to obtain a homogeneous melt should be chosen when transparent glasses are sought [103].

Note that the presented reactions in this paper also occur when using AlN, which is the other commonly used nitride for oxynitride glasses synthesis. When the system is at equilibrium, the nitrogen pressure resulting from AlN decomposition into aluminum and molecular nitrogen is lower than the one resulting from Si_3N_4 decomposition into silicon and molecular nitrogen, whatever the temperature [107]. Therefore, there should be less metallic micro-particles in the glasses when using AlN, meaning they should be more transparent. However, the consequences of using AlN over Si_3N_4 changes with the synthesis conditions of the glass: it may provide a clearer glass [103], have no effect on the transparency [90], or oppositely remain undissolved in the glass [72] [110] as its melting temperature is higher, making the choice of the nitride more complicated than expected.

Beside Si_3N_4 and AlN, the use other nitrides was reported such as Li_3N, Ca_3N_2, TiN, YN, NbN, Ba_3N_2 or the Si_2N_2O oxynitride alternatively [22] [111] [112] [113], but they may present various drawbacks: Mg_3N_2, Ca_3N_2, Ba_3N_2, LaN and Li_3N are hygroscopic, while some are difficult to prepare [114] [115].

To summarize, the most suitable nitride must fulfil several requirements: i) reduce as few oxides as possible, *i.e.* the Gibbs free energy of the oxidation reaction of a nitride AN_x into its oxide AO_y ($\frac{2}{y}\,AN_x + O_2 \longrightarrow \frac{2}{y}\,AO_y + \frac{x}{y}\,N_2$) must be higher than the Gibbs free energies of the

$\frac{2}{y}$ M + O_2 = $\frac{2}{y}$ MO_y reactions of the oxides composing the glass (where M is a metal). Note that in a few cases, an oxide can be nitrided rather than reduced by Si_3N_4, which in a Ti-oxynitride glass led to the crystallization of TiN [21]. ii) It must melt in the usual temperature range of the syntheses when mixed with the other precursors, and be soluble in the glass to obtain a glass-matrix free from heterogeneities iii) but not decompose according to previously presented side reactions, and specifically the Gibbs free energy of the $\frac{2}{x}$ AN_x $\longrightarrow$ $\frac{2}{x}$ A + N_2 reaction must be positive over the temperature range of the syntheses in order to prevent the formation of metallic micro-particles and the loss of N_2. These conditions must also be considered when using metals or hydrides as reactants, as they will form nitrides upon heating in a N_2 atmosphere.

It should be noted that the loss of transparency that is often observed in oxynitride glasses containing more than 15 eq. % N, is more likely to result from impurities and side reactions occurring in the melt, such as the reduction of silicon to form transition metal silicide nanoparticles, rather than from the incorporation of nitrogen in the glass network itself [62].

b) Chemical composition

Oxides

There are sometimes weight losses that are not anticipated by the Ellingham diagrams. For example, weight losses of MgO [62 116], SrO [9], CaO [68], BaO [7], Y_2O_3 and Al_2O_3 [117] were reported and were found to increase with the temperature, the nitrogen content and the holding time. Weight losses in Na and B were also reported, as their corresponding oxides, Na_2O and B_2O_3, are prone to volatilization at high temperatures [37 38 40 108], and because Na_2O is reduced by Si_3N_4 at temperatures above 850 K (Fig 5). However, several authors reported no significant loss of Na despite close experimental conditions [6 8].

Fluorine

Fluorine is found to decrease the viscosity of the oxynitride melt, thus easing homogenization, to decrease both T_g and T_c temperatures, and to increase the solubility of nitrogen. In addition, the incorporation of fluorine widens the chemical range of glass formation, decreases the melting point of the reactants mixture, with a negligible incidence on hardness and elastic moduli [118 119 120]. However, the use of fluorides may lead to the crystallization of NaF and CaF_2, to demixing and to loss of Si in the form of SiF_4 gas, which is detrimental to the environment [121 122]. The latter can be prevented by choosing a glass composition where Al-F bonds are favored over Si-F bonds [123].

Rare-earths

The use of rare-earths in oxynitride glasses leads to an increase in T_c, T_g, and in an increase in hardness and Young's modulus [18 28 124 125], which are found to increase with the cationic field strength (*CFS*) of the rare-earths, itself depending on their coordination number [126]: $CFS = \frac{z}{r^2}$, where z is the ion charge and r the ionic radii. Indeed, rare-earths show a strong *CFS*, thus enhancing the stacking density and leading to a more rigid system. The change of the thermal expansion coefficient with the *CFS* is not linear [18]. In the search for stiff and hard glasses, yttrium has been the most widely investigated rare-earth.

4 STRUCTURE AND PHYSICAL PROPERTIES

4.1 Incorporating nitrogen into the atomic network of glasses

a) Silicates

The atomic structure of glasses is of paramount importance to understand the macroscopic properties. Early studies show that nitrogen is incorporated into the atomic network by substituting oxygen, thus increasing the crosslinking because of its larger coordination number [127] according to:

338 $$\equiv Si–O–Si\equiv \longrightarrow \equiv Si–N\begin{matrix} \diagup\ Si\equiv \\ \diagdown\ Si\equiv \end{matrix} \qquad (20)$$

339 In fact, nitrogen-containing gaseous species such as NH_3 or molecular N_2 that are present
340 in the synthesis environment were not detected in oxynitride glasses [46 49 128]. It was proposed
341 that the substitution of oxygen by nitrogen benefits from the fact that Si-N and Si-O bond
342 lengths are very close [26]. For example, the average values of the Si-N and Si-O bond lengths
343 were estimated in a Y-Ba-Si-O-N glass by neutron diffraction experiments, and are centered on
344 1.72 and 1.61 Å respectively [129]. Slightly different values, but close to each other, were reported
345 for a Na-Si-O-N glass [130]. Although nitrogen atoms are mainly bridging, non-bridging nitrogen
346 ($\equiv Si\text{-}N^{-}\text{-}Si\equiv$) and possibly double non-bridging nitrogen ($\equiv Si\text{-}N^{2-}$) exist as well [127 129 131 132],
347 thus forming bonds with other cations such as rare-earths [126 133 134]. The average coordination
348 number of nitrogen ranges between 2 and 3, with three-fold coordinated nitrogen atoms being
349 predominant over two-fold coordinated ones [127 129]. In oxynitride glasses obtained via the
350 ammonolysis route, NH and NH_2 groups exist in the glass when the ammonolysis is uncomplete
351 [39 135 136].

352 Silicon in oxynitride glasses is 4-fold coordinated to both oxygen and nitrogen, hence
353 leading to structural units such as SiO_4, SiO_3N, SiO_2N_2, and $SiON_3$ [137 138]. Although the
354 presence of SiN_4 structural units could not be evidenced by means of Magic-Angle Spinning
355 solid-state Nuclear Magnetic Resonance spectroscopy (*MAS-NMR*) [137], such units may survive
356 due to the incomplete dissolution of the Si_3N_4 nitrogen precursors. The connected Q^n units
357 (where n is the number of bridging anions coordinated to a cation tetrahedron Q) form sheet,
358 chain and cycle structures in the glass network [126]. Their relative populations vary with the
359 chemical composition of the glasses. The incorporation of nitrogen induces the formation of
360 $Si(O, N)_4$ mixed tetrahedra [120 126 137 139 140]. At low nitrogen content, SiO_3N units are the most

frequently encountered whereas SiO_2N_2 tetrahedra become predominant at large nitrogen content. The $SiON_3$ population is usually small. Therefore, a typical silicon oxynitride glass network consists of Si-O-Si and Si-N-Si linkages [126 137]. It is not excluded that the structure of nitrogen-rich oxynitride glasses obtained using metals or hydrides as reactants differs from the one of glasses obtained by conventional melting of oxides and nitrides and quenching, but further studies are required to clarify this point [12].

b) Phosphates

Phosphate-based oxynitride glasses are composed of various species including orthophosphate $[PO_4]^{3-}$ [35], pyrophosphate $[P_2O_7]^{4-}$ [35 49 141], oligophosphate $[P_nO_{3n+1}]^{-n-2}$ [142] and metaphosphate $[P_nO_{3n}]^{-n}$, where n is the number of PO_4 tetrahedra in the chain [35 143]. The Q^n units in phosphate glasses show linkages such as Q^3-Q^3, Q^2-Q^2, and Q^2-Q^1 indicating a glass network consisting of reticulated parts, chains and/or rings [142] where two different kinds of nitrogen atoms are encountered, namely two-fold nitrogen N_d (– N =) and three-fold nitrogen N_t (– N<). The way nitrogen substitutes for oxygen is presented in Fig. 6 [46 49 144]. In the first case (Fig. 6a), the substitution of $\frac{2}{3}N_d$ requires 1 NBO (= O) double-bonded to a phosphorus atom, while in the second one (Fig. 6b) the substitution of $\frac{1}{3}N_d$ requires $\frac{1}{2}$ bridging-oxygen (BO) (– O –). Terminating OH groups are not considered due to their low concentration [145]. Two rules can then be deduced from these schemes: i) $N_d = 1NBO + \frac{1}{2}BO$, and ii) $N_t = \frac{3}{2}BO$. The N_t and N_d populations follow the same trend no matter the system. There is slightly more N_t than N_d with increasing nitrogen content, up to the point where the N_t population seems to reach a limit corresponding to one N_t per tetrahedron [146], while the N_d population becomes predominant and increases even more [43 46 95]. The N_t/N_d ratio was found close to 3 no matter the N/P ratio in ref. [145]. It is suggested that nitrogen substitutes randomly for oxygen in the glass to form PO_3N units

[146]. Then, the observed fraction of $P(O, N)_4$ mixed tetrahedra suggests that nitrogen preferentially substitutes for oxygen atoms bridging PO_4 and PO_3N units [146 147], which are hence changed to PO_3N and PO_2N_2 units as illustrated in Fig. 7. As nitrogen enters the network, the PO_4 population drastically decreases, while the PO_2N_2 population and mostly the PO_3N population increase with increasing nitrogen content [43 45 145 146 95 148]. The PO_3N population increases up to some equilibrium fraction, while the PO_2N_2 population keeps increasing. This matches the proposed mechanism, where firstly PO_3N tetrahedra are formed at the expense of PO_4 tetrahedra, and then connected PO_4-PO_3N tetrahedra are converted to PO_3N-PO_2N_2 tetrahedra [148], finally resulting in homogenously distributed oxynitride micro-domains. A different mechanism is proposed in lead-containing glasses, where PO_4 tetrahedra close to lead atoms are preferentially nitrided into PO_3N tetrahedra [43 148]. Phosphorus oxynitride glasses are thus based on PO_4, PO_3N and PO_2N_2 units. The PO_3N and PO_2N_2 units can be sub-divided into various sub-units, that are distinguishable by means of *NMR* [142]: PO_3N(a): P connected to 2 *BO*, 1 *NBO* and 1 N (N_t or N_d); PO_3N(b): P connected to 1 *BO*, 2 *NBO* and 1 N (N_t or N_d); PO_3N(c): P connected to 0 *BO*, 3 *NBO* and 1 N (N_t or N_d); PO_2N_2(a): P connected to 1 *BO*, 1 *NBO* and 2 N (N_t or N_d); and PO_2N_2(b): P connected to 0 *BO*, 2 *NBO* and 2 N (N_t or N_d). Although PON_3 and PN_4 tetrahedra are found in compounds such as P_4ON_6 [149], such units were not reported in oxynitride glasses so far. This is because at large N/P ratio, crystallization occurs and prevents the formation of such units. Some papers focused on mixed M-Si-P-O-N oxynitride glasses [33 35], which present P-O-Si linkages as well as traces of 6-fold coordinated silicon atoms. It was suggested that the content in SiO_6 octahedra decreases with increasing nitrogen content. Moreover, it appears that P-N bonds form preferentially with respect to Si-N bonds.

c) Borates

Investigations into boron-containing oxynitride glasses are very limited and therefore little is known about such materials. When boron is incorporated by means of a sol-gel route, B-N bonds form at the expense of Si-O-B linkages [39 40]. Such bond formation was not confirmed in glasses made by the conventional melting route. Whether $B(O, N)_x$ units exist, with x being equal to 3 and/or 4 depending on the boron atoms coordination number (3 or 4), or whether isolated BN units form still remain to be elucidated [38 40]. In view of the low solubility of BN in oxide melts the latter hypothesis is more likely [59].

d) Aluminosilicates

Aluminum is mostly 4-fold coordinated in oxynitride aluminosilicate glasses. However, a fraction of the Al atoms (about one third in *RE*-Mg-Si-Al-O-N glasses) is present in higher coordination states (up to 5-6) [137 140]. The larger the nitrogen content is, and the larger the 6-fold aluminum content becomes [150]. Although aluminum can form bonds with nitrogen, Si-N bonds form preferentially over Al-N bonds [137]. Nevertheless, solid-state *NMR* investigations brought to light the existence of AlO_3N structural units in addition to the AlO_4 tetrahedra [137]. Besides, the formation of AlO_2N_2 and $AlON_3$ was evidenced in oxynitride glass-ceramics [151], but not in oxynitride glasses though. Nevertheless, it is noteworthy that these latter structural units are hardly detectable because of the quadrupolar broadening of the peaks in solid-state *NMR* [150 152]. Therefore, aluminosilicate oxynitride glasses are composed of Al-O-Al and Si-O-Al linkages, while Al-N-Al and/or Si-N-Al linkages are expected as a result of mixed $Al(O, N)_4$ tetrahedra [126 137]. In phosphate-based glasses, aluminum is also present in AlO_4 AlO_5 and AlO_6 polyhedra [153], forming Al-O-P linkages [33 72], but there is no certainty regarding the existence of Al-N bonds in such glasses.

433 e) Fluorine

434 Few studies dealing with oxyfluoronitride glasses were reported [24 31 67]. In phosphate-based
435 oxynitride glasses, fluorine can form P-F bonds, thus acting as a depolymerization agent leading
436 to $P(O, F)_4$ and $P(O, N, F)_4$ units. The formation of PO_2FN units was suggested [154]. Fluorine
437 can also be linked to *M* cations such as Na or Ca, thus forming compounds such as CaF_2 [155 156].
438 In the case of aluminosilicates glasses, an increase in fluorine leads to an increase in Al(V) and
439 Al(VI) at the expense of Al(IV) [31 157]. A few possible reasons could be that a fraction of the
440 aluminum forms $Al[O_xF_y]^{n-}$ oxyfluorides complexes. The presence of nitrogen does not seem
441 to change the fluorine environment. In fact, the effects of nitrogen and fluorine on the properties
442 of such glasses seem additive and independent [67 120] .

443 f) Sulfur

444 New mixed oxy-sulfide nitride glasses (MOSN), obtained from the ammonolysis of oxy-sulfide
445 phosphate melts, where nitrogen substitutes for both oxygen and sulfur, were investigated in
446 the past few years [158 159 160]. These glasses, which combine high ionic conductivities, suitability
447 for thin film processing, resistance toward devitrification and chemical durability, are
448 promising materials as solid state electrolytes in all solid state batteries. Their structure is
449 chiefly based on mixed $P(O, S, N)_4$ tetrahedra.

450 g) Rare-earths

451 Rare-earths (*RE*) in glasses are characterized by their high coordination states [18 126 161]. In the
452 case of oxynitride glasses, the impacts of nitrogen and rare-earths on their properties are
453 additive and independent [125]. *RE* cations are mainly bonded to oxygen and found in a +3
454 oxidation state, with the exception of europium, which also occurs in a +2 oxidation state.
455

h) Miscellaneous: Be, Mg, Ge

A recent study in Be-containing oxynitride glasses showed that beryllium is present as BeO_4 structural units, having a similar role to that of aluminum [8]. This results in Si-O-Be linkages. There is no evidence for a bonding between Be and N. The coordination number of magnesium is usually high in oxynitride glasses (>4) [162]. However, depending on the chemical composition, a fraction of the magnesium atoms exists as MgO_4 structural units, thus forming Mg-O-Si linkages [126 140 162 163]. The addition of more nitrogen into the glasses leads to an increase of the amount of 4-fold magnesium [162]. However, Mg-N bonds were not reported so far in oxynitride glasses. The structure of germanophosphate oxynitride glasses was recently investigated [77]. Germanium is present in GeO_4, GeO_5 and GeO_6 polyhedra that mostly forming Ge-O-P linkages (rather than Ge-O-Ge linkages). Nitrogen substitution has various effects on their structures: It preferentially substitutes Ge-O-P linkages to form Ge-O-Ge linkages and mixed $P(O, N)_4$ tetrahedra, and depolymerizes both the phosphate and the germanate network, as GeO_4 tetrahedra becomes the most predominant germanium-based polyhedra. Whether germanium form Ge-N bonds, or solely bonds to oxygen to form GeO_x units (x equal to 4, 5 and/or 6) remains to be elucidated.

4.2 Physical properties

Oxynitride glasses exhibit higher T_g and T_c, and a lower thermal expansion coefficient than their oxide counterparts [22 26]. They further show up with a larger refractive index [10 22], ionic conductivity (in particular in the Na-Si-O-N [101], Li-Si-O-N [64] and Li-P-O-N [51] systems), dielectric constant [164 165 166], and density [26]. Some minor change of the heat capacity were also reported [167 168]. Nitrogen also improves the corrosion resistance in water [169 94] as well as in acidic or alkali media [127 170]. It seems that the incorporation of nitrogen has little effect on the cytotoxicity of the glasses [36], but slightly reduces the bioactivity [120 171]. Moreover, oxynitride

glasses present a reducing character because of the N^{3-}/N^0 redox couple, that causes either the nitridation of various oxides or their reduction into metallic or inter-metallic particles (such as iron-silicides), which is a likely source for the loss of transparency [172] [173] [174]. The reducing character of the nitrided melt was studied both in phosphorous and in silicon oxynitride glasses [115], and explains the reduction of Eu^{3+} to Eu^{2+} in an europium-doped Y-Si-Al-O-N oxynitride glass [175]. Furthermore, rare-earth containing oxynitride glasses exhibit luminescent properties [76] [175] [176]. The concept of optical basicity was extended to oxynitride glasses and a linear relationship was found between the anionic polarizability (O^{2-} and N^{3-} anions) and the composition [177]. The introduction of nitrogen into the melt results in increases of the shear viscosity [169] and of the surface tension [178]. The viscosity of oxynitride liquids is mostly very sensitive to temperature [77] [147]. For examples, Y-Si-Al-O-N and Ca-Si-Al-O-N glass forming liquids can be considered as relatively "fragile" per the C.A. Angell classification [179], as will be discussed in § 5.4. However, this trend does not apply to all systems and the fragility index is found to decrease with the N/P ratio in LiPON and NaPON glasses [147], while it increases with the N/P ratio in LiNaGePON glasses [77].

The biocompatibility and enhanced durability of silicon oxynitride glass systems is of paramount interest for biomedical applications as bioactive oxide glasses suffer from relatively small strength, hardness and stiffness, which prevent applications in major load-bearing applications. In such a field of applications, the improvement of the mechanical performance induced by the substitution of oxygen by nitrogen is decisive.

5 MECHANICAL PROPERTIES

The mechanical properties of oxynitride glasses are mostly directly correlated to their nitrogen content. Hardness, elastic moduli, fracture toughness and viscosity increase with the nitrogen content, no matter the system [22] [26] [44] [53] [58] [105] [180]. Since the Si-N bond is weaker than the Si-O

bond, the atomic packing density and the fine details of the atomic arrangement, including the increase of the cross-linking, come into play. In contrast with the case of silicon oxynitride glasses (SiON), the mechanical properties of phosphorus oxynitride glasses (PON) were scarcely reported and are thus discarded in the following paragraphs. Nevertheless, PON follow the same general trends as SiON: the introduction of nitrogen increases hardness, stiffness, chemical durability, resistance to stress corrosion, toughness and strength. In the case of PON glasses, which exhibit relatively low T_g and mechanical performance and are particularly sensitive to humidity, the substitution of oxygen by nitrogen results in a dramatic and often critical improvement of the mechanical properties and durability, hence enlarging the field of applications for human bone replacements, metal sealing (thanks to relatively large expansion coefficients) or solid electrolytes for rechargeable batteries. For PON, K is typically between 30 and 35 GPa, E is between 35 and 45 GPa, and H is between 1.5 and 2.5 GPa.

5.1 Elastic moduli and Poisson's ratio

Oxynitride glasses possess the largest elastic moduli among non-metallic glasses, with E reaching about 190 GPa (SiYAlON system). The bulk modulus of a material can be seen as reflecting a volume density of energy. This is expressed by what is known as the 1st Grüneisen rule: $K=\frac{mnU_o}{9V_o}$, where U_o is the atomic bonding energy, V_o the atomic volume at equilibrium, and m and n are the power law exponents of the pair potential,

$$U(r) = \frac{nU_o}{(m-n)}\left[\left(\frac{r_o}{r}\right)^m - \frac{m}{n}\left(\frac{r_o}{r}\right)^n\right] \qquad (21)$$

This expression can be extended to a multicomponent glass composition using the average dissociation enthalpy $< U_0 >$ and the volume $< V_0 >$ of an equivalent mole of glass (also referred to as an *atom gram*) (see ref. [23] for details). The dissociation enthalpy was calculated for many glasses from different chemical systems, including metallic ones, and is shown in Fig. 8 as a

function of the glass transition temperature. In the same way that the shear modulus of crystalline materials is found to scale with the melting point, $<U_0>$ is found to increase with T_g. However, the energy range for silicon oxynitride glasses (from 550 to 700 kJ·mol^{-1}) is quite close to the one for silicate glasses, and there is no one to one relationship between elastic moduli and T_g for glasses, as shown in Fig. 9. In fact, the Si-N bond is weaker than the Si-O one, and much larger than metallic bonds, but metallic glasses appear to compete well with oxynitride ones, whereas silicate glasses are usually less rigid. For example, K reaches values as large as 139 and 159 GPa for $Y_{0.146}Si_{0.232}Al_{0.034}O_{0.31}N_{0.29}$ and $Pd_{0.4}Cu_{0.3}Ni_{0.1}P_{0.2}$ glasses respectively. For vitreous silica, $K \approx 33$ GPa. The reason for this counter-intuitive observation lies in the fact that the atomic packing efficiency (C_g) is much larger ($< V_0 >$ is smaller) in metallic glasses than in non-metallic ones, and furthermore that it is larger in silicon oxynitride glasses than in oxide silicates. In the case of a disordered arrangement of atoms, C_g can be determined from the ratio of the effective volume occupied by a mole of atoms (V_0), as estimated from the atomic radii ($V_0 = \mathcal{N}\sum_i \frac{4}{3}\pi x_i r_i^3$, where $\mathcal{N}$ is Avogadro number and x_i and r_i are the atomic fraction and ionic radius of the i^{th} element), to the corresponding volume of glass, calculated from the specific mass of the glass (ρ) and the molar mass of the constituents (m_i):

$$C_g = \frac{\mathcal{N}\ \sum_i (4/3)\pi\ x_i r_i^3}{(\sum_i x_i m_i)/\rho} \qquad (22)$$

The atomic packing density typically ranges between 0.45 and 0.55 for silicate glasses, between 0.57 and 0.65 for silicon oxynitride ones and reaches values as large as 0.8 in precious metal based metallic glasses. Therefore, an efficient atomic packing is found to compensate easily for a relatively small energy content. Consistently with a large packing density, oxynitride glasses show up with relatively large values for ν, typically around 0.26-0.32, whereas for oxide silicates ν is between 0.15 (a-SiO_2) and 0.25 (Fig. 10). The increase in

553 Young's modulus is roughly linear with the nitrogen content and given by: E(GPa) = E_0+4xN
554 (at.%), where E_0 is Young's modulus of the parent oxide glass (Fig. 11).

555 Makishima and Mackenzie (*M-M*) [181] proposed a model to estimate the elastic moduli
556 from the packing density, C_g, the molar fraction, f_i, and the volume density of energy, ΔH_{ai}^V (J.m^{-3}),
557 of the i^{th} oxide entering the glass composition. For instance, in the case of Young's modulus,
558 these authors arrived at the following expression: $E=2C_g \sum f_i \Delta H_{ai}^V$, where ΔH_{ai} is calculated
559 from the molar dissociation energy (J·mol^{-1}), the specific mass, ρ_i, and the molar mass, M_i,
560 according to $\Delta H_{ai}^V = \frac{\rho_i}{M_i} \Delta H_{ai}$ [23]. Values for C_g obtained this way are mostly close to experimental
561 data in the case of silicate glasses, but are greatly underestimated in the case of oxynitride
562 glasses. An extension of this theory was proposed, using the ratio of formation free energies of
563 monoatomic nitrogen on oxygen in their gaseous state at 298.15 K $\frac{\Delta G_{f(Ng)}^{\circ}}{\Delta G_{f(Og)}^{\circ}} = \frac{108.99}{54.99} = 1.98$, in order
564 to take into account the energetic stabilization excess induced by the substitution of nitrogen in
565 the glass network [182]. Thus, when the i^{th} compound of the glass is a nitride, the volume density
566 of energy is calculated such as $\Delta H_{ai}^V = 1.98 \frac{\rho_i}{M_i} \Delta H_{ai}$, leading to better agreements with measured
567 Young's moduli of oxynitride glasses. Nevertheless, these models are chiefly empirical and
568 hardly help understand what is going on when compositional changes occur. Furthermore, such
569 theoretical calculations require the knowledge of the actual value for the glass density (C_g
570 determination), so that the ab initio character is somewhat lost. As was underlined by Daucé et
571 al. [183] a reliable quantitative estimation based on the *M-M*-type approach is only possible for
572 glasses with compositions close to those of crystallized compounds for which the actual ionic
573 radii are accurately known. Furthermore, the dissociation energy is not a reticular energy and it
574 is not obvious that C_g can be used as an ersatz of the Madelung constant. Back to the simple
575 extension of the Grüneisen model, it turns out that for silicon oxynitride glasses, K increases
576 rather exponentially with the volume density of energy (Fig. 12). As far as the change in the

ionic radii and interatomic bonding energy with composition can be neglected, this suggests a monotonic increase of the mn product with the nitrogen content. This is likely due to the marked increase of C_g with the nitrogen content, which would result in a steeper repulsive branch for the pair potential, that is in an increase of m. Interestingly, a large slope for the K versus $< U_0 > /< V_0 >$ correlation was also noticed for germanate and silico-aluminate glasses, where Ge and Al are known to experience 4, 5 and 6-fold coordination, which is a favorable situation toward an efficient packing. The mn product is close to 9 for phosphate and alkali-alkaline-earth silicate glasses, but is larger for metallic glasses [184] and for germanates and aluminates [23].

5.2 Hardness, indentation deformation and indentation cracking

The hardness (H) of silicon oxynitride glasses ranges between 6 and 13 GPa (Vickers indentation tests) and make these glasses the hardest of all glasses (Fig. 13). The largest values were reported for Rare-earth-Si-Al-O-N glasses (especially with yttrium). For a given system, H is found to increase almost linearly with the nitrogen content, with $H \approx H_0 + \alpha$[N] (e/o) where α ranges from 0.07 to 0.12 [185] (Fig. 14), where H_0 is the hardness of the parent oxide glass. The reason for oxynitride glasses being so hard is two-fold: i) the atomic network cross-linking degree is large thanks to 3-fold coordinated nitrogen, and ii) atoms are more efficiently packed in average in the presence of nitrogen. The combination of these two factors compensates for the Si-N bond being weaker than the Si-O bond. The effect of the average crosslinking degree on hardness was addressed by means of the topological constraints theory [185] and it was found that hardness increases linearly with the number of additional constraints Δn induced by the substitution of nitrogen. Since Δn increases linearly with the nitrogen content in e/o, this provides an explanation for the linear relationship between H and N e/o. Furthermore, according to this model the slope depends little on the composition of the parent nitrogen free glass. For

oxynitride glasses, the E/H ratio is typically in the 11-13 range, and ν is between 0.26 and 0.32. This makes these glasses sensitive to lateral (subsurface) and to radial cracking under a sharp indenter, as opposed to cone and median cracking (see Fig. 9 in ref. [186]) (Fig 15). Besides, because C_g is relatively large in such glasses, there is little room for stress accommodation through densification (as in the case of silica-rich glasses for example). Hence, in spite of the fact that silicon oxynitride glasses are stiff, hard, strong, and relatively tough (see next paragraph), they experience a well-developed radial crack system (Fig. 16).

5.3 Fracture toughness and slow crack growth

The fracture toughness of silicon oxynitride glasses, as estimated by means of indentation-cracking techniques (mostly), is in between 0.6 and 2.7 MPa·$\sqrt{m}$ [187 188 65 189 190 191 192 193 194], and increases with the nitrogen content (Fig. 16). The incorporation of 15 e/o N in an oxide silicate glass typically results to a 10-15 % increase of K_{Ic}. Nevertheless, the actual increase, as measured by means of a self-consistent method, such as the Single Edge Precracked Beam (*SEPB*) or the Chevron-Notch (*CN*), is usually smaller [195]. A relatively simple approach to predicting the fracture surface energy, γ, in a quantitative manner from the stoichiometric composition consists in assuming a propagating crack extends following a path disrupting the weakest links of the energy landscape and to estimate the surface energy from the bond strength and the bond concentration along this fracture surface [194]. The fracture toughness, K_{Ic}, is then deduced by means of the classical expression from linear fracture mechanics: $K_{Ic}=\sqrt{\frac{2\gamma E}{1-\nu^2}}$. Let x_i be the stoichiometric fraction of the species involved in the i^{th} diatomic bonding energy U_{oi} (in J·mol^{-1}), between the i^{th} cation and a first neighbor oxygen anion in the case of an oxide glass, and let n_i be the number of such bonds supposed to be broken as the crack front propagates to the next unit, then γ is expressed as

$$\gamma = \frac{1}{2}\,(\sum_i 4/3\pi\, x_i r_i^3)^{-2/3} \mathcal{N}^{-1} {C_g}^{2/3}\ < U_o > \quad (23)$$

where ρ and M_o are the glass density (specific mass) and the molar mass of a representative unit (gram-atom of glass), $\mathcal{N}$ is Avogadro number, and the ½ prefactor on the right hand side member accounts for the fact that the bond disruption process leads to the formation of two complementary surfaces (a crack has two walls) (see ref. [194] for details).

For example, Young's modulus as high as 150 GPa is typically measured for glasses from the *RE*-Si-Al-O-N system (*RE*: Y, Nd, Lu etc.). In such glasses, the mean energy ($< U_o >$ $<U_o>=\sum_i x_i\, n_i U_{oi}$), is calculated considering the number of Si-N bonds, taken as ¾ x_N, and the remaining Si-O bonds equal to $x_{Si} - ¾\, x_N$. For example, for the $Y_{0.123}Si_{0.185}Al_{0.07}O_{0.547}N_{0.075}$ glass composition, taking $U_{o\text{Si-N}}$, $U_{o\text{Al-O}}$, $U_{o\text{Y-O}}$ equal to 437, 502 and 698 kJ·mol^{-1} respectively, a fracture energy of 4.0 J.m^{-2} and a theoretical toughness of 1.2 MPa·$\sqrt{m}$ are calculated, quite close to the experimental value of 1.05 MPa·$\sqrt{m}$[103]. The theoretical values are in the range 0.8-1.1 MPa·$\sqrt{m}$ for oxynitride glasses (Fig. 16) and are close to the experimental values as obtained by the *SEPB* or by the *CN* method, but about twice smaller than the ones obtained by the indentation cracking method at large nitrogen content. It is thus concluded that the toughness of silicon oxynitride glasses with 5 to 20 at.% nitrogen is near 1 MPa·$\sqrt{m}$. In oxynitride glasses, calculations were performed considering nitrogen is three-fold coordinated and solely bonded to silicon, even though a non-negligible amount of Al-N bonds exists in such glasses [137]. When Poisson's ratio ν was not specified, a value of 0.28 was arbitrarily chosen as Poisson's ratio often ranges from 0.26 to 0.32 in silicon oxynitride glasses [65 189 188] (Fig. 10).

Silicon oxynitride glass is also present at the grain-boundaries in Si_3N_4-based ceramics, due to the liquid phase that forms in the high temperature sintering conditions thanks to the sintering additives (Al_2O_3, Y_2O_3 etc.). In these ceramics, a fracture toughness as large as 4-5 MPa·$\sqrt{m}$ is obtained by controlling i) the size and the morphology of the elongated grains and

650 ii) the composition and crystallinity of the secondary grain boundary phase [196]. The theoretical
651 approach introduced above results in a K_{Ic} value of about 1.44 MPa·$\sqrt{m}$ for Si_3N_4 (ν = 0.28 and
652 E = 300 GPa). This value is in agreement with the experimental one obtained for Si_3N_4 single
653 crystal, that is regardless of any additional toughening phenomena such as crack deflection and
654 crack front bowing due to the acicular shape of the β-Si_3N_4 grains, which lies between 1.5 and
655 2.0 MPa·$\sqrt{m}$ [197]. This value can thus be seen as an optimum value for a straight through crack
656 in a silicon nitride material.
657 The introduction of nitrogen in a silicate or a phosphate glass was found to increase the
658 chemical durability and the resistance to environmentally assisted slow crack growth (known
659 as the stress corrosion phenomenon). The study by Bhatnagar et al [189] reveals a decrease of the
660 crack growth velocity for a given stress intensity factor by over an order of magnitude in an Y-
661 Si-Al-O-N glass in comparison to soda-lime-silica and borosilicate glasses in air, and an
662 improvement of several orders of magnitude in water. Coon [198] studied the slow crack growth
663 resistance of a Y-Si-Al-O-N glass by means of the double cantilever beam technique, and
664 concluded to a several orders of magnitude smaller crack velocity at a given stress intensity
665 factor for the oxynitride glass in comparison to a standard glass slide (likely a soda-lime-silica
666 glass). Besides, the stress corrosion exponent (Paris law exponent) is typically above 150 for
667 the oxynitride glass and below 150 for the oxide silicate glass.
668
669 **5.4 High temperature behaviour**
670 a) Elasticity
671 In all cases but a-SiO_2 (and to a minor extent SiOC glass), the temperature dependence of the
672 elastic moduli of glass exhibits a transition range between a slow softening rate and a faster
673 one, corresponding to the glass transition (Fig. 17). The glass transition temperatures as well as
674 the room temperature values of E and μ, and the softening rate immediately above T_g

675 ($dE/dT(T_g^+)$ and $d\mu/dT(T_g^+)$, i.e., in the supercooled liquid range, are reported in Table I. Glass
676 transition temperatures as measured from $E(T)$ curves are usually smaller by 10 to 20 K than
677 the ones obtained by dilatometry with the same heating rate. There seems to be two kinds of
678 behavior. For relatively stiff glasses such as oxynitride ones, and for $T_g < T < 1.1T_g$ [23]:

679 $$E / E(T_g) = T_g / T \qquad (24)$$

680 In most cases, the shear modulus, which depends more on T than E, changes with T above T_g
681 according to a power law expression [199] (Fig. 18):

682 $$\mu / \mu(T_g) = (T_g / T)^{\alpha} \qquad (25)$$

683 where α ranges between 0.07 (a-SiO_2) and 9 (oxynitride glass) for the selected glass
684 composition summarized in Table I. A value of 10 was reported for a-Se [199].
685 The temperature dependence of the elastic moduli reflects the degree of ''fragility'' (as defined
686 by Angell [200]) of the liquid. Therefore, with α equal to 9 (and a fragility index, m, equal to 48),
687 silicon oxynitride liquids show up as particularly fragile. In polycrystalline ceramics with glassy
688 grain-boundary phases obtained by liquid-phase sintering, the fast softening observed beyond
689 T_g is solely due to the effect of the liquid grain boundary films and pockets (see ref. [201] for a
690 review on this problem). Amorphous silica exhibits an anomalous behavior characterized by a
691 rising shear modulus in the [0.5-0.95] range for T/T_g ($d\mu/dT(T_g^-) = 3.1$ MPa·K^{-1}) and a strong
692 resistance to de-structuration above T_g as evidenced by a remarkably slow softening
693 ($d\mu/dT(T_g^+) = -5.3$ MPa·K^{-1}) and by the fact that ν remains almost constant from 0.5 to 1.2 T_g,
694 suggesting that the liquid keeps a strong memory of the atomic structure of the glassy solid,
695 with little changes of the average coordination and dimensionality throughout the glass
696 transition range. On the contrary to a-SiO_2, oxynitride glasses soften rapidly with rising
697 temperature in spite of a relatively high degree of interatomic connectivity, high T_g and large
698 elastic moduli. This suggests that the oxynitride glass network consists of stiff (likely nitrogen-

699 rich) structural units embedded in a weaker phase (likely concentrating impurities, and alkaline
700 and alkaline-earth species). Recalling that ν shows up as a mirror of the overall network
701 connectivity, then the dramatic decrease of $\mu(T)$ (faster than for glycerol!) with respect to $E(T)$
702 and the corresponding rapid increase in $\nu(T)$ — comparing with those of organic liquids such
703 as bitumen or glycerol — is an indication of the dramatic network de-structuration above T_g.
704
705 b) Viscosity
706 The glass transition range is associated with a shear viscosity coefficient of 10^{12}-$10^{12.6}$ Pa·s. In
707 the case of silicon oxynitride glasses, and in particular those containing rare earth, T_g is in
708 between 1123 and 1273 K (Fig. 19), which makes these glasses more refractory than silicate
709 and aluminosilicate glasses in the transition range, approaching the viscosity of a-SiO_2 for the
710 largest nitrogen content. The viscosity increases typically by three orders of magnitude as the
711 nitrogen content is raised by about 25 e/o N (about 11 at.% N). Nevertheless, the apparent
712 activation (Q) energy for viscous flow, which can be obtained straightforwardly from an
713 Arrhenius modelling of the temperature dependence of the viscosity ($\eta = \eta_0 \exp[Q/(RT)]$), is
714 exceptionally large, typically between 800 and 1200 kJ·mol^{-1} in the transition range. A striking
715 value of 2100 kJ·mol^{-1} was once reported for a $Ca_{11.04}Si_{10}O_{13.21}N_{11.8}$ glass ($T_g \approx 1010$ °C,
716 58 e/o N) [202]. In view of the great sensitivity to temperature change of the mechanical properties
717 of oxynitride glass forming liquids, such as the elastic moduli and the viscosity coefficient,
718 these liquids can be considered as particularly fragile ones. Indeed, the fragility index of
719 oxynitride glasses, as defined by $m = \mathrm{d}\log_{10}\eta/\mathrm{d}(T(\eta=10^{12}\ \text{Pa·s})/T) \approx Q/(2.303RT_g)$, ranges
720 typically from 47 to 55 ($m \approx 18$ for a-SiO_2) (Fig. 20).
721 The apparent activation energy for creep of silicon nitride-based ceramics reported by most of
722 the authors roughly coincides with the activation energy for viscous flow (above T_g) of an
723 oxynitride glass containing the same elements as the sintering aids used for the liquid phase

sintering. This result confirms the major importance of the glassy phase on the creep behavior of these ceramic materials.

6. GLASS-CERAMICS & COMPOSITES

The crystallization of oxynitride glasses was studied in various glass systems, and especially in *RE*-Si-Al-O-N ones. In most cases, devitrification occurs through a self-nucleation process, which was attributed to the presence of metallic nano/micro particles resulting from the decomposition of Si_3N_4 [4] [203]. The crystal growth rate was observed to decrease with increasing nitrogen content in Li-Si-O-N glasses, likely because of the increase cross-linking and stability of the glass network in the presence of nitrogen [204] [205].

A change in the nitrogen source (AlN or Si_3N_4) leads to different crystalline phases [151] [206]. Nitrogen is eventually found to have some incidence on both the relative fractions and the structures of the different phases [206] [207]. Depending on the composition, nitrogen may either not enter the crystallized phases [100] [205] or lead to the crystallization of oxynitrides [151] [187] [208] [209] [118] [210] [211] or nitrides (such as ZrN) [212]. The elastic moduli, hardness and fracture toughness of the resulting oxynitride glass ceramics are typically improved by 25% in comparison to the oxynitride parent glass [187] [213].

A few composites based on oxynitride glasses were reported. SiC/Y-Mg-Si-Al-O-N composites present increased Young's modulus, fracture toughness and hardness compared to the SiC-free glassy matrix [214] [215]. The higher the volume fraction of the SiC particles and the smaller their size, the stronger the increase. Alternatively, SiC fibres were incorporated in a Y-Si-Al-O-N glass, which was then crystallized [216]. Si-Al-Ca-O-N oxynitride glass fibres were used as reinforcements in various oxide glasses [217] or in aluminum alloys [218]. Si_3N_4 particles were dispersed or grown in various oxynitride glasses, such as *RE*-Mg-Si-O-N [219] and Y-Si-Al-O-N [220] [221]. TiN/Y-Mg-Si-Al-O-N composites were synthesized by nitriding in the melt a

748 TiO_xN_y oxynitride using AlN, and showed a great increase in Young's modulus, shear modulus,
749 hardness and fracture toughness with increasing vol.% of TiN [115].

750

751 ## 7. MOLECULAR SIMULATIONS AND *AB INITIO* MOLECULAR ORBITAL
752 CALCULATIONS

753 Very few molecular simulations of oxynitride glasses were reported. One focused on the Na-
754 Si-O-N system and showed similar trends in density and in mechanical properties with
755 increasing nitrogen content as measured experimentally [131]. It was also proposed here that *NBN*
756 result from the substitution of *NBO* with nitrogen. Another paper focused on the (Sc)-(Y)-(La)-
757 Mg-Si-O-N system, and observed close radial distribution function (*RDF*) with experimental
758 data, but with some discrepancies especially on the glasses structure [222].

759 *Ab initio* molecular orbital calculations were performed to determine the interatomic
760 potential, the bending force constant and the stretching force constant of several glass model
761 molecules for silicon oxynitride glasses [223]. It would appear that while the stretching force
762 constant (Si-N) of the model molecules decreases with increasing nitrogen content, the bending
763 force constant (Si-N-Si) oppositely increases. A simple model to calculate the bulk modulus
764 shows a stronger effect of the bending force constant over the stretching force constant, which
765 could be a reason among others explaining why oxynitride glasses show stronger bulk modulus
766 than their oxide counterparts.

767

768 ## 8. CONCLUSIONS AND PERSPECTIVES

769 The unique mechanical properties of oxynitride glasses make them special glasses. Their
770 Young's modulus is typically above 100 GPa, their hardness above 8 GPa and their toughness
771 greater than 1 MPa·$\sqrt{m}$. By combining these properties with functional properties in the fields
772 of optics, biomaterials, chemical reactivity or electricity, these specialty glasses appear suitable

for various applications in solid-state batteries, because of their strong ionic conductivity, as biomaterials for bone replacement, for special windows, coatings and reinforcement fibres thanks to their hardness, stiffness and chemical inertia, for innovative enamels [134] and for nuclear waste vitrification [63].

Nevertheless, oxynitride glasses are disadvantaged by their difficulty and their cost of production, inherent in the high temperatures required, typically above 1600° C for the melting step, in the use of nitrogen compounds and in the control of the atmosphere. Besides, in spite of notable progress in this area, the incorporation of nitrogen mostly results in the loss of transparency.

There remain several fundamental questions regarding the atomic arrangement in oxynitride glasses. In particular, the role of alkaline and alkaline-earth cations and the way nitrogen is connected to the structural units, such as $(Si, Al)(O, N)_4$ tetrahedra, remains to be elucidated. While nitrogen is lighter than oxygen and increases the cross-linking, oxynitride glasses are denser that than their parent oxide glasses, exhibit a larger atomic packing density, a larger Poisson's ratio, and are stiffer and harder despite the Si-N bond being weaker than the Si-O one. Further structural investigations, in conjunction with molecular dynamic simulation, are required to get a better insight into the atomic scale structure of these glasses.

ACKNOWLEDGEMENTS

We acknowledge financial support from Région Bretagne and from the European Research Council (ERC Adv. Grant "DAMREG"). We are indebted to Jean Rocherullé for fruitful discussions.

ORCID

Alexis Duval iD https://orcid.org/0000-0001-9192-2454

Patrick Houizot iD https://orcid.org/0000-0002-6360-6996

Tanguy Rouxel iD https://orcid.org/ 0000-0002-9961-2458

REFERENCES

1. Hampshire S. Nitride Ceramics. Ed. by R. W. Cahn, P. Haasen and E. J. Kramer, In Materials Science and Technology, vol. 11, 119-171; 1994 https://doi.org/https://doi.org/10.1002/9783527603978.mst0119
2. Morkoç H. General Properties of Nitrides. In: Nitride Semiconductors and Devices. Springer Series in Materials Science, Springer, Berlin, Heidelberg; 1999 https://doi.org/10.1007/978-3-642-58562-3_2
3. Mulfinger H-O. Physical and Chemical Solubility of Nitrogen in Glass Melts. *J Am Ceram Soc*. 1966;49(9):462–467. https://doi.org/10.1111/j.1151-2916.1966.tb13300.x
4. Hampshire S, Pomeroy MJ. Oxynitride Glasses. *Encycl Glas Sci Technol Hist Cult Ed by P Richet, R Conradt, A Tak J Dyon*. 2021;Wiley(1st ed):891–900. https://doi.org/https://doi.org/10.1002/9781118801017.ch7.8
5. Loehman RE. Preparation and Properties of Oxynitride Glasses. *J Non Cryst Solids*. 1983;56(1–3):123–134. https://doi.org/10.1016/0022-3093(83)90457-X
6. Unuma H, Komori K, Sakka S. Electrical Conductivity and Chemical Durability in Alkali-Silicate Oxynitride Glasses. *J Non Cryst Solids*. 1987;95–96:913–920. https://doi.org/10.1016/S0022-3093(87)80698-1
7. Sharafat A, Jonson B. Glasses in the Ba-Si-O-N System. *J Am Ceram Soc*. 2011;94(9):2912–2917. https://doi.org/10.1111/j.1551-2916.2011.04718.x
8. Wójcik NA, Jonson B, Möncke D, *et al.* The Effect of Nitrogen on the Structure and Thermal Properties of Beryllium-Containing Na-(Li)-Si-O-N Glasses. *J Non Cryst Solids*. 2019;522(July):119585. https://doi.org/10.1016/j.jnoncrysol.2019.119585
9. Sharafat A, Forslund B, Grins J, Esmaeilzadeh S. Formation and Properties of Nitrogen-Rich Strontium Silicon Oxynitride Glasses. *J Mater Sci*. 2009;44(2):664–670. https://doi.org/10.1007/s10853-008-3058-3

826 10. Sharafat A, Grins J, Esmaeilzadeh S. Hardness and Refractive Index of Ca-Si-O-N
827 glasses. *J Non Cryst Solids*. 2009;355(4–5):301–304.
828 https://doi.org/10.1016/j.jnoncrysol.2008.11.019
829 11. Shaw TM, Thomas G, Loehman RE. Formation and Microstructure of Mg-Si-O-N
830 Glasses. *J Am Ceram Soc*. 1984;67(10):643–647. https://doi.org/10.1111/j.1151-
831 2916.1984.tb19674.x
832 12. Hakeem AS, Grins J, Esmaeilzadeh S. La-Si-O-N Glasses. Part I. Extension of the
833 Glass Forming Region. *J Eur Ceram Soc*. 2007;27(16):4773–4781.
834 https://doi.org/10.1016/j.jeurceramsoc.2007.04.002
835 13. Murakami Y, Akiyama K, Yamamoto H. Phase Relation and Properties of Oxynitride
836 Glasses in the Si3N4-Yb2O3-SiO2 System. *J Mater Sci Lett*. 1996;15(14):1271–1272.
837 https://doi.org/10.1007/BF00274398
838 14. Hakeem AS, Ali S, Jonson B. Preparation and Properties of Mixed La-Pr Silicate
839 Oxynitride Glasses. *J Non Cryst Solids*. 2013;368(1):93–97.
840 https://doi.org/10.1016/j.jnoncrysol.2013.03.013
841 15. Tredway WK, Risbud SH. Melt Processing and Properties of Barium-Sialon Glasses. *J*
842 *Am Ceram Soc*. 1983;66(5):324–327. https://doi.org/10.1111/j.1151-
843 2916.1983.tb10041.x
844 16. Sakka S, Kamiya K, Yoko T. Preparation and Properties of Ca-Al-Si-O-N Oxynitride
845 Glasses. *J Non Cryst Solids*. 1983;56(1–3):147–152. https://doi.org/10.1016/0022-
846 3093(83)90460-X
847 17. Ramesh R, Nestor E, Pomeroy MJ, Hampshire S. Formation of Ln-Si-Al-O-N Glasses
848 and their Properties. *J Eur Ceram Soc*. 1997;17(15–16):1933–1939.
849 https://doi.org/10.1016/s0955-2219(97)00057-5
850 18. Menke Y, Peltier-Baron V, Hampshire S. Effect of Rare-Earth Cations on Properties of

Sialon Glasses. *J Non Cryst Solids*. 2000;276(1):145–150. https://doi.org/10.1016/S0022-3093(00)00268-4

19. Pomeroy MJ, Nestor E, Ramesh R, Hampshire S. Properties and Crystallization of Rare-Earth Si-Al-O-N Glasses Containing Mixed Trivalent Modifiers. *J Am Ceram Soc*. 2005;88(4):875–881. https://doi.org/10.1111/j.1551-2916.2004.00141.x

20. Becher PF, Ferber MK. Temperature-Dependent Viscosity of SiREAl-Based Glasses as a Function of N:O and RE:Al Ratios (RE = La, Gd, Y, and Lu). *J Am Ceram Soc*. 2004;87(7):1274–1279. https://doi.org/10.1111/j.1151-2916.2004.tb07722.x

21. Wakihara T, Tatami J, Komeya K, *et al.* Effect of TiO2 Addition on Thermal and Mechanical Properties of Y-Si-Al-O-N Glasses. *J Eur Ceram Soc*. 2012;32(6):1157–1161. https://doi.org/10.1016/j.jeurceramsoc.2011.12.002

22. Garcia ÀR, Clausell C, Barba A. Oxynitride glasses: A review. *Bol la Soc Esp Ceram y Vidr*. 2016;55(6):209–218. https://doi.org/10.1016/j.bsecv.2016.09.004

23. Rouxel T. Elastic Properties and Short-to Medium-Range Order in Glasses. *J Am Ceram Soc*. 2007;90(10):3019–3039. https://doi.org/10.1111/j.1551-2916.2007.01945.x

24. Clausell C, Barba A, Jarque JC, García-Bellés ÁR, Pomeroy MJ, Hampshire S. Compositional Effects on the Crosslink Density of Ca–(Mg)–(Y)–Si–Al–Oxyfluoronitride Glasses. *J Am Ceram Soc*. 2018;101(1):189–200. https://doi.org/10.1111/jace.15210

25. Pomeroy MJ, Mulcahy C, Hampshire S. Independent Effects of Nitrogen Substitution for Oxygen and Yttrium Substitution for Magnesium on the Properties of Mg-Y-Si-Al-O-N Glasses. *J Am Ceram Soc*. 2003;86(3):458–464. https://doi.org/10.1111/j.1151-2916.2003.tb03321.x

26. Loehman RE. Oxynitride Glasses. *J Non Cryst Solids*. 1980;42:433–446.

https://doi.org/10.1016/0022-3093(80)90042-3

27. Becher PF, Lance MJ, Ferber MK, Hoffmann MJ, Satet RL. The Influence of Mg Substitution for Al on the Properties of SiMeRE Oxynitride Glasses. *J Non Cryst Solids*. 2004;333(2):124–128. https://doi.org/10.1016/j.jnoncrysol.2003.09.044

28. Lofaj F, Hvizdoš P, Dorčáková F, Satet R, Hoffmann MJ, de Arellano-López AR. Indentation Moduli and Microhardness of RE-Si-Mg-O-N Glasses (RE = Sc, Y, La, Sm, Yb and Lu) with Different Nitrogen Content. *Mater Sci Eng A*. 2003;357(1–2):181–187. https://doi.org/10.1016/S0921-5093(03)00170-9

29. Lofaj F, Satet R, Hoffmann MJ, de Arellano López AR. Thermal Expansion and Glass Transition Temperature of the Rare-Earth Doped Oxynitride Glasses. *J Eur Ceram Soc*. 2004;24(12):3377–3385. https://doi.org/10.1016/j.jeurceramsoc.2003.10.012

30. Sharafat A, Grins J, Esmaeilzadeh S. Properties of High Nitrogen Content Mixed Alkali Earth Oxynitride Glasses (AExCa1-x)1.2(1)SiO1.9(1)N0.86(6), AE = Mg, Sr, Ba. *J Non Cryst Solids*. 2009;355(22–23):1259–1263. https://doi.org/10.1016/j.jnoncrysol.2009.04.036

31. Hanifi AR, Genson A, Pomeroy MJ, Hampshire S. Independent but Additive Effects of Fluorine and Nitrogen Substitution on Properties of a Calcium Aluminosilicate Glass. *J Am Ceram Soc*. 2012;95(2):600–606. https://doi.org/10.1111/j.1551-2916.2011.05001.x

32. Coon DN, Doyle TE, Weidner JR. Refractive Indices of Glasses in the Y-Al-Si-O-N System. *J Non Cryst Solids*. 1989;108(2):180–186. https://doi.org/10.1016/0022-3093(89)90581-4

33. Kidari A, Mercier C, Leriche A, Revel B, Pomeroy MJ, Hampshire S. Synthesis and Structure of Na-Li-Si-Al-P-O-N Glasses Prepared by Melt Nitridation using NH3. *Mater Lett*. 2012;84:38–40. https://doi.org/10.1016/j.matlet.2012.06.029

34. Wójcik NA, Jonson B, Möncke D, *et al.* Influence of Synthesis Conditions on Glass Formation, Structure and Thermal Properties in the Na2O-CaO-P2O5 System Doped with Si3N4 and Mg. *J Non Cryst Solids*. 2018;494(January):66–77. https://doi.org/10.1016/j.jnoncrysol.2018.04.055

35. Paraschiv GL, Muñoz F, Tricot G, *et al.* Mixed Alkali Silicophosphate Oxynitride Glasses: Structure-Property Relations. *J Non Cryst Solids*. 2017;462:51–64. https://doi.org/10.1016/j.jnoncrysol.2017.02.011

36. Mabrouk A, Bachar A, Atbir A, *et al.* Mechanical Properties, Structure, Bioactivity and Cytotoxicity of Bioactive Na-Ca-Si-P-O-(N) glasses. *J Mech Behav Biomed Mater*. 2018;86:284–293. https://doi.org/10.1016/j.jmbbm.2018.06.023

37. Jankowski PE, Risbud SH. Formation and Characterization of Oxynitride Glasses in the Si-Ca-Al-O-N and Si-Ca-Al,B-O-N systems. *J Mater Sci*. 1983;18(7):2087–2094. https://doi.org/10.1007/BF00555002

38. Coon DN, Rapp JG, Bradt RC, Pantano CG. Mechanical Properties of Silicon-Oxynitride glasses. *J Non Cryst Solids*. 1983;56(1–3):161–165. https://doi.org/10.1016/0022-3093(83)90462-3

39. Brinker CJ, Haaland DM. Oxynitride Glass Formation from Gels. *J Am Ceram Soc*. 1983;66(11):758–765. https://doi.org/10.1111/j.1151-2916.1983.tb10558.x

40. Brinker CJ, Haaland DM, Loehman RE. Oxynitride Glasses Prepared from Gels and Melts. *J Non Cryst Solids*. 1983;56(1–3):179–184. https://doi.org/10.1016/0022-3093(83)90465-9

41. Brow RK, Peng YB, Day DE. Properties and Structure of P-O-N-H Glasses. *J Non Cryst Solids*. 1990;126(3):231–238. https://doi.org/10.1016/0022-3093(90)90824-6

42. Cicconi MR, Veber A, de Ligny D, Rocherullé J, Lebullenger R, Tessier F. Chemical Tunability of Europium Emission in Phosphate Glasses. *J Lumin*. 2017;183:53–61.

https://doi.org/10.1016/j.jlumin.2016.11.019

43. Muñoz F, Pascual L, Durán A, *et al.* Structural Study of Phosphorus Oxynitride Glasses LiNaPbPON by Nuclear Magnetic Resonance and X-Ray Photoelectron Spectroscopy. *J Non Cryst Solids*. 2003;324(1–2):142–149. https://doi.org/10.1016/S0022-3093(03)00171-6

44. Yung H, Shih PY, Liu HS, Chin TS. Nitridation Effect On Properties of Stannous-Lead Phosphate Glasses. *J Am Ceram Soc*. 1997;80(9):2213–2220. https://doi.org/10.1111/j.1151-2916.1997.tb03110.x

45. Hémono N, Rocherullé J, Le Floch M, Muñoz F. Synthesis and Characterization of SnO-Containing Phosphorous Oxynitride Glasses. *J Non Cryst Solids*. 2008;354(17):1822–1827. https://doi.org/10.1016/j.jnoncrysol.2007.10.014

46. Marchand R, Agliz D, Boukbir L, Quemerais A. Characterization of Nitrogen Containing Phosphate Glasses by X-Ray Photoelectron Spectroscopy. *J Non Cryst Solids*. 1988;103(1):35–44. https://doi.org/10.1016/0022-3093(88)90413-9

47. Lei X, Day DE. Preparation and Properties of Oxynitride Glasses Made from Potassium Metaphosphate. *J Am Ceram Soc*. 1989;72(9):1601–1603. https://doi.org/10.1111/j.1151-2916.1989.tb06289.x

48. Su Y, Falgenhauer J, Polity A, *et al.* LiPON Thin Films with High Nitrogen Content for Application in Lithium Batteries and Electrochromic Devices Prepared by RF Magnetron Sputtering. *Solid State Ionics*. 2015;282:63–69. https://doi.org/10.1016/j.ssi.2015.09.022

49. Day DE. Structural Role of Nitrogen in Phosphate Glasses. *J Non Cryst Solids*. 1989;112(1–3):7–14. https://doi.org/10.1016/0022-3093(89)90488-2

50. Lee SJ, Bae JH, Lee HW, Baik HK, Lee SM. Electrical Conductivity in Li-Si-P-O-N oxynitride Thin-Films. *J Power Sources*. 2003;123(1):61–64.

https://doi.org/10.1016/S0378-7753(03)00457-9

51. Muñoz F, Durán A, Pascual L, Montagne L, Revel B, Rodrigues ACM. Increased Electrical Conductivity of LiPON Glasses Produced by Ammonolysis. *Solid State Ionics*. 2008;179(15–16):574–579. https://doi.org/10.1016/j.ssi.2008.04.004

52. Park C, Lee S, Choi S, Shin D. Effect of Boron/Phosphorus Ratio in Lithium Boron Phosphorus Oxynitride Thin Film Electrolytes for All-Solid-State Thin Film Batteries. *Thin Solid Films*. 2019;685(September 2018):434–439. https://doi.org/10.1016/j.tsf.2019.06.055

53. Muñoz F, Saitoh A, Jiménez-Riobóo RJ, Balda R. Synthesis and Properties of Nd-Doped Oxynitride Phosphate Laser Glasses. *J Non Cryst Solids*. 2017;473(July):125–131. https://doi.org/10.1016/j.jnoncrysol.2017.08.005

54. Hamon Y, Vinatier P, Kamitsos EI, *et al.* Nitrogen Flow Rate as a New Key Parameter for the Nitridation of Electrolyte Thin Films. *Solid State Ionics*. 2008;179(21–26):1223–1226. https://doi.org/10.1016/j.ssi.2008.04.005

55. Dussauze M, Kamitsos EI, Johansson P, *et al.* Lithium Ion Conducting Boron-Oxynitride Amorphous Thin Films: Synthesis and Molecular Structure by Infrared Spectroscopy and Density Functional Theory Modeling. *J Phys Chem C*. 2013;117(14):7202–7213. https://doi.org/10.1021/jp401527x

56. Beier W, Krüner G, Frischat GH. Different Ways to Incorporate Nitrogen in Li_2O-B_2O_3 Glasses. *Defect Diffus Forum*. 1987;53–54:387–392. https://doi.org/10.4028/www.scientific.net/ddf.53-54.387

57. Nakane S, Kobayashi Y, Yoshinaka M, Hirota K, Yamaguchi O. A Novel Synthesis of B-Al-Ca-O-(N) Glasses by Self-Propagating High-Temperature Combustion Method. *Mater Res Bull*. 2007;42(1):46–55. https://doi.org/10.1016/j.materresbull.2006.05.012

58. Krüner G, Frischat GH. Some Properties of N-Containing Lithium Borate Glasses

Prepared by Different Sol-Gel Methods. *J Non Cryst Solids*. 1990;121(1–3):167–170. https://doi.org/10.1016/0022-3093(90)90125-6

59. Wakasugi T, Tsukihashi F, Sano N. The solubilities of BN in B. *J Non Cryst Solids*. 1991;135:139–145. https://doi.org/10.1016/0022-3093(91)90414-2

60. Wakasugi T, Tsukihashi F, Sano N. Thermodynamics of Nitrogen in B2O3, B2O3─SiO2, and B2O3─CaO Systems. *J Am Ceram Soc*. 1991;74(7):1650–1653. https://doi.org/10.1111/j.1151-2916.1991.tb07154.x

61. Bagaasen LM, Risbud SH. Silicon-Free Oxynitride Glasses Via Nitridation of Aluminate Glassmelts. *J Am Ceram Soc*. 1983;66(4):C-69-C-71. https://doi.org/10.1111/j.1151-2916.1983.tb15700.x

62. Ali S, Jonson B, Pomeroy MJ, Hampshire S. Issues Associated with the Development of Transparent Oxynitride Glasses. *Ceram Int*. 2015;41(3):3345–3354. https://doi.org/10.1016/j.ceramint.2014.11.030

63. Das T. Oxynitride glasses - an overview. *Bull Mater Sci*. 2000;23(6):499–507. https://doi.org/10.1007/BF02903891

64. Singh SP, Schneider JF, Kundu S, *et al.* Structure and Ionic Conductivity of Nitrated Lithium Disilicate (LiSiON) Glasses. *Mater Chem Phys*. 2018;211:438–444. https://doi.org/10.1016/j.matchemphys.2018.02.045

65. Homeny J, Paulik SW. High-Pressure Synthesis of Mg-Al-Si-O-N Oxynitride Glasses. *Mater Lett*. 1990;9:504–507. https://doi.org/10.1016/0167-577X(90)90096-5

66. Redington W, Redington M, Hampshire S. Effect of Cooling Rate on Glass Formation for Some Oxynitride Glasses. *Mater Sci Forum*. 2007;554:25–30. https://doi.org/10.4028/www.scientific.net/msf.554.25

67. García-Bellés A, Clausell C, Barba A, Pomeroy MJ, Hampshire S. Effect of Fluorine and Nitrogen Content on the Properties of Ca-Mg-Si-Al-O-(N)-(F) Glasses. *Ceram Int*.

2017;43(5):4197–4204. https://doi.org/10.1016/j.ceramint.2016.12.046

68. Sharafat A, Grins J, Esmaeilzadeh S. Glass-Forming Region in the Ca-Si-O-N system Using CaH2 as Ca Source. *J Eur Ceram Soc*. 2008;28(14):2659–2664. https://doi.org/10.1016/j.jeurceramsoc.2008.04.017

69. Hakeem AS, Daucé R, Leonova E, *et al.* Silicate Glasses with Unprecedented High Nitrogen and Electropositive Metal Contents Obtained by Using Metals as Precursors. *Adv Mater*. 2005;17(18):2214–2216. https://doi.org/10.1002/adma.200500715

70. Mittl JC, Tallman RL, Kelsey PV, Jolley JG. HIP Glassmaking for High Nitrogen Compositions in the Y-Si-Al-O-N. *J Non Cryst Solids*. 1985;71:287–294. https://doi.org/10.1016/0022-3093(85)90298-4

71. Marchand R. Nitrogen-Containing Phosphate Glasses. *J Non Cryst Solids*. 1983;56(1–3):173–178. https://doi.org/10.1016/0022-3093(83)90464-7

72. Kidari A, Pomeroy MJ, Hampshire S. Novel Na-Li-SiAlPON Glasses Prepared by Melt Synthesis Using AlN. *J Eur Ceram Soc*. 2012;32(7):1389–1394. https://doi.org/10.1016/j.jeurceramsoc.2010.12.034

73. Peng YB, Day DE. Factors Affecting Nitrogen Dissolution in Sodium Metaphosphate Glass. *J Am Ceram Soc*. 1987;70(4):232–236. https://doi.org/10.1111/j.1151-2916.1987.tb04973.x

74. Sauze A Le, Marchand R. Chemically Durable Nitrided Phosphate Glasses Resulting from Nitrogen/Oxygen Substitution within PO4 Tetrahedra. *J Non Cryst Solids*. 2000;263:285–292. https://doi.org/10.1016/S0022-3093(99)00673-0

75. Ecolivet C, Boukbir L, Marchand R. Brillouin Scattering Investigation of Phosphorus Oxynitride Glasses. *Mater Chem Phys*. 1989;21(2):191–199. https://doi.org/10.1016/0254-0584(89)90113-2

76. Muñoz F, Jiménez-Riobóo RJ, Balda R. Chemical and Structural Heterogeneities in

Nd-Doped Oxynitride Phosphate Laser Glasses. *J Alloys Compd*. 2020;816:152657. https://doi.org/10.1016/j.jallcom.2019.152657

77. Paraschiv GL, Muñoz F, Jensen LR, Larsen RM, Yue Y, Smedskjaer MM. Structural Impact of Nitrogen Incorporation on Properties of Alkali Germanophosphate Glasses. *J Am Ceram Soc*. 2018;101(11):5004–5019. https://doi.org/10.1111/jace.15747

78. Kamiya K, Ohya M, Yoko T. Nitrogen-Containing SiO2 Glass Fibers Prepared by Ammonolysis of Gels Made from Silicon Alkoxides. *J Non Cryst Solids*. 1986;83:208–222. https://doi.org/10.1016/0022-3093(86)90068-2

79. Belot V, Corriu R, Leclercq D, Mutin PH, Vioux A. Preparation of Oxynitride Silicon Glasses. Nitridation of Functional Silica Xerogels. *J Non Cryst Solids*. 1992;147–148(C):309–312. https://doi.org/10.1016/S0022-3093(05)80635-0

80. Muñoz F, Benne D, Pascual L, *et al.* Silicon Oxynitride Glasses Produced by Ammonolysis from Colloidal Silica. *J Non Cryst Solids*. 2004;345–346:647–652. https://doi.org/10.1016/j.jnoncrysol.2004.08.163

81. Ahmadi S, Eftekhari Yekta B, Sarpoolaky H, Aghaei A. Preparation of Monolithic Oxynitride Glasses by Sol-Gel Method. *J Non Cryst Solids*. 2014;404:61–66. https://doi.org/10.1016/j.jnoncrysol.2014.07.037

82. Szaniawska K, Murawski L, Pastuszak R, Walewski M, Fantozzi G. Nitridation and Densification of SiO2 Aerogels. *J Non Cryst Solids*. 2001;286(1–2):58–63. https://doi.org/10.1016/S0022-3093(01)00478-1

83. Sekine M, Katayama S, Mitomo M. Preparation of Silicon Oxynitride Glass Fibers by Ammonolysis of Silica Gels. *J Non Cryst Solids*. 1991;134(3):199–207. https://doi.org/10.1016/0022-3093(91)90377-I

84. Mutin PH. Control of the Composition and Structure of Silicon Oxycarbide and Oxynitride Glasses Derived from Polysiloxane Precursors. *J Sol-Gel Sci Technol*.

1999;14(1):27–38. https://doi.org/10.1023/A:1008769913083

85. Deckwerth M, Rüssel C. Oxynitride Glasses in the System Mg-Ca-Al-Si-O-N Prepared with the Aid of a Polymeric Precursor: Preparation and Properties. *J Non Cryst Solids*. 1997;217(1):66–71. https://doi.org/10.1016/S0022-3093(97)00150-6

86. Moriceau J. Élaboration de Vitrocéramiques et de Composites Particulaires à Matrice Vitreuse aux Propriétés Mécaniques et Fonctionnelles Innovantes. *PhD Thesis, Univ Rennes 1*. 2018.

87. Wang GX, Lu GQ, Pei B, Yu AB. Oxidation Mechanism of Si3N4-Bonded SiC Ceramics by CO, CO2 and Steam. *J Mater Sci*. 1998;33(5):1309–1317. https://doi.org/10.1023/A:1004354415867

88. Wusirika R. Problems Associated with the Melting of Oxynitride Glasses. *J Am Ceram Soc*. 1984;67(11):c232–c233. https://doi.org/10.1111/j.1151-2916.1984.tb19492.x

89. Riley FL. Nitrogen Ceramics. Ed. by F. L. Riley, Noordhoff Pub; 1977

90. Korgul P, Thompson DP. The Transparency of Oxynitride Glasses. *J Mater Sci*. 1993;28(2):506–512. https://doi.org/10.1007/BF00357831

91. Grieveson P. Nitrogen Ceramics. Ed. by F. L. Riley, Noordhoff Pub; 1977

92. Segawa H, Hirosaki N, Ohki S, Deguchi K, Shimizu T. Exploration of Metaphosphate Glasses Dispersed with Eu-Doped SiAlON for White LED Applications. *Opt Mater (Amst)*. 2015;42:399–405. https://doi.org/10.1016/j.optmat.2015.01.036

93. Rajaram M, Day DE. Nitrogen Dissolution in Alkali-Barium-Metaphosphate Melts. *J Mater Sci*. 1989;24(2):573–576. https://doi.org/10.1007/BF01107444

94. Bunker BC, Arnold GW, Rajaram M, Day DE. Corrosion of Phosphorus Oxynitride Glasses in Water and Humid Air. *J Am Ceram Soc*. 1987;70(6):425–430. https://doi.org/10.1111/j.1151-2916.1987.tb05663.x

95. Le Sauze A, Montagne L, Palavit G, Marchand R. Nitridation of Alkali Metaphosphate

Glasses: A Comparative Structural Analysis of the Na-P-O-N and Li-Na-P-O-N Systems. *J Non Cryst Solids*. 2001;293–295(1):81–86. https://doi.org/10.1016/S0022-3093(01)00655-X

96. Ott D, Raub CJ. The Affinity of the Platinum Metals for Refractory Oxides. *Platin Met Rev*. 1976;20(3):79–85.

97. Riguidel Q, Muñoz F. Effect of nitridation on the aqueous dissolution of Na2O-K 2O-CaO-P2O5 metaphosphate glasses. *Acta Biomater*. 2011;7(6):2631–2636. https://doi.org/10.1016/j.actbio.2011.03.025

98. Rajaram M, Day DE. Cation Effects in NaPO3 Glasses Doped with Metal Nitrides and Oxides. *J Am Ceram Soc*. 1986;69(5):400–403. https://doi.org/10.1111/j.1151-2916.1986.tb04768.x

99. Oota M, Kanamori T, Kitamura S, *et al.* Decrease of Silicon Defects in Oxynitride Glass. *J Non Cryst Solids*. 1997;209(1–2):69–75. https://doi.org/10.1016/S0022-3093(96)00546-7

100. Tredway WK, Risbud SH. Preparation and Controlled Crystallization of Si-Ba-Al-O-N Oxynitride Glasses. *J Non Cryst Solids*. 1983;56(1–3):135–140. https://doi.org/10.1016/0022-3093(83)90458-1

101. Unuma H, Sakka S. Electrical Conductivity in Na-Si-O-N Oxynitride Glasses. *J Mater Sci Lett*. 1987;6(9):996–998. https://doi.org/10.1007/BF01729111

102. Dériano S, Rouxel T, Malherbe S, Rocherullé J, Duisit G, Jézéquel G. Mechanical Strength Improvement of a Soda-Lime-Silica Glass by Thermal Treatment Under Flowing Gas. *J Eur Ceram Soc*. 2004;24(9):2803–2812. https://doi.org/10.1016/j.jeurceramsoc.2003.09.019

103. Messier DR, Deguire EJ. Thermal Decomposition in the System Si-Y-AI-O-N. *J Am Ceram Soc*. 1984;67(9):602–605. https://doi.org/10.1111/j.1151-2916.1984.tb19602.x

104. Batha HD, Whitney ED. Kinetics and Mechanism of the Thermal Decomposition of Si3N4. *J Am Ceram Soc*. 1973;56(7):365–369. https://doi.org/10.1111/j.1151-2916.1973.tb12687.x

105. Ding Y, Ding Z, Jiang Z. Formation and Properties of Y-Al-Si-O-N Glasses in the Grain Boundaries of Si3N4 Ceramics. *J Non Cryst Solids*. 1989;112:408–412. https://doi.org/10.1016/0022-3093(89)90563-2

106. Messier DR, Gazza GE. Thermal Decomposition of Al2O3-Si3N4 Mixtures. *J Am Ceram Soc*. 1975;58(11–12):538–540. https://doi.org/10.1111/j.1151-2916.1975.tb18789.x

107. Sunggi B, Rishi R. Suppression of Frothing by Silicon Addition During Oxynitride Glass Synthesis. *J Am Ceram Soc*. 1985;68(7):C-168-C-170. https://doi.org/10.1111/j.1151-2916.1985.tb10161.x

108. Wusirika RR, Chyung CK. Oxynitride Glasses and Glass-Ceramics. *J Non Cryst Solids*. 1980;38–39:39–44. https://doi.org/10.1016/0022-3093(80)90391-9

109. Bachar A, Mercier C, Tricoteaux A, *et al.* Effect of Nitrogen on Properties of Na2O-CaO-SrO-ZnO-SiO2 Glasses. *J Am Ceram Soc*. 2015;98(3):748–757. https://doi.org/10.1111/jace.13361

110. Ali S, Hakeem AS, Höche T, Drmosh QA, Khan AA, Jonson B. Investigation of Instinctive Defects in Nitrogen Enrich Lanthanum Silicon Oxynitride Glasses. 2020;1–21. https://doi.org/10.21203/rs.3.rs-22643/v1

111. Reidmeyer MR, Day DE. Preparation and Properties of Nitrogen-Doped Phosphate Glasses. *J Am Ceram Soc*. 1985;68(8):C-188-C-190. https://doi.org/10.1111/j.1151-2916.1985.tb10177.x

112. Fletcher JP, Risbud SH, Hayashi S, Kirkpatrick RJ. Structural Investigation of Oxyfluoronitride Glasses. *Defect Diffus Forum*. 1987;53–54:493–500.

https://doi.org/10.4028/www.scientific.net/ddf.53-54.493

113. Glasses and Glass-Ceramics. Ed. by M. H. Lewis, Chapman and Hall (London); 1989

114. Avignon-Pocquillon L. Préparation et Caractérisation de Nouveaux Matériaux Azotés : i. Composés à Structure Tétraédrique; ii. Composites à Matrice Verre. *PhD Thesis, Univ Rennes 1*. 1989.

115. Turmel J-M. Etude de Réactions d'Oxydoréduction dans des Verres Oxyazotés. Application à la Réduction d'Oyxdes Métalliques et à l'Obtention de Composites Particulaires Verre-Nitrure de Titane. *PhD Thesis, Univ Rennes 1*. 1997.

116. Ali S, Jonson B. Compositional Effects on the Properties of High Nitrogen Content Alkaline-Earth Silicon Oxynitride Glasses, AE=Mg, Ca, Sr, Ba. *J Eur Ceram Soc*. 2011;31(4):611–618. https://doi.org/10.1016/j.jeurceramsoc.2010.11.005

117. Shillito KR, Wills RR, Bennett RB. Silicon Metal Oxynitride Glasses. *J Am Ceram Soc*. 1978;61(11–12):537–537. https://doi.org/10.1111/j.1151-2916.1978.tb16143.x

118. Luo Z, Lu A, Qu G, Lei Y. Synthesis, Crystallization Behavior, Microstructure and Mechanical Properties of Oxynitride Glass-Ceramics with Fluorine Addition. *J Non Cryst Solids*. 2013;362(1):207–215. https://doi.org/10.1016/j.jnoncrysol.2012.11.048

119. Hanifi AR, Genson A, Pomeroy MJ, Hampshire S. Oxyfluoronitride Glasses with High Elastic Modulus and Low Glass Transition Temperatures. *J Am Ceram Soc*. 2009;92(5):1141–1144. https://doi.org/10.1111/j.1551-2916.2009.03041.x

120. Bachar A, Mercier C, Tricoteaux A, Hampshire S, Leriche A, Follet C. Effect of Nitrogen and Fluorine on Mechanical Properties and Bioactivity in Two Series of Bioactive Glasses. *J Mech Behav Biomed Mater*. 2013;23:133–148. https://doi.org/10.1016/j.jmbbm.2013.03.010

121. Hanifi AR, Genson A, Pomeroy MJ, Hampshire S. A New Generation of Oxynitride Glasses Containing Fluorine. *Iran J Mater Sci Eng*. 2010;7(1):15–23.

122. Hampshire S, Hanifi AR, Genson A, Pomeroy MJ. Ca-Si-Al-O-N Glasses: Effects of Fluorine on Glass Formation and Properties. *Key Eng Mater*. 2007;352:165–172. https://doi.org/10.4028/www.scientific.net/kem.352.165

123. García-Bellés AR, Monzõ M, Barba A, *et al.* Properties of Ca-(Y)-Si-Al-O-N-F Glasses: Independent and Additive Effects of Fluorine and Nitrogen. *J Am Ceram Soc*. 2013;96(4):1131–1137. https://doi.org/10.1111/jace.12249

124. Ohashi M, Nakamura K, Hirao K, Kanzaki S, Hampshire S. Formation and Properties of Ln-Si-O-N Glasses (Ln = Lanthanides or Y). *J Am Ceram Soc*. 1995;78(1):71–76. https://doi.org/10.1111/j.1151-2916.1995.tb08362.x

125. Lofaj F, Dériano S, LeFloch M, Rouxel T, Hoffmann MJ. Structure and Rheological Properties of the RE-Si-Mg-O-N (RE = Sc, Y, La, Nd, Sm, Gd, Yb and Lu) Glasses. *J Non Cryst Solids*. 2004;344(1–2):8–16. https://doi.org/10.1016/j.jnoncrysol.2004.07.018

126. Becher PF, Hampshire S, Pomeroy MJ, Hoffmann MJ, Lance MJ, Satet RL. An Overview of the Structure and Properties of Silicon-Based Oxynitride Glasses. *Int J Appl Glas Sci*. 2011;2(1):63–83. https://doi.org/10.1111/j.2041-1294.2011.00042.x

127. Sakka S. Structure, Properties and Application of Oxynitride Glasses. *J Non Cryst Solids*. 1995;181(3):215–224. https://doi.org/10.1016/S0022-3093(94)00514-1

128. Reidmeyer MR, Day DE. Phosphorus Oxynitride Glasses. *J Non Cryst Solids*. 1995;181(3):201–214. https://doi.org/10.1016/S0022-3093(94)00511-7

129. Jin JS, Kozuka H, Yoko T, Fukunaga T. Structure of Y-Ba-Si-O-N Glasses by Neutron Diffraction. *Phys Status Solidi*. 1996;193:295–306. https://doi.org/10.1002/pssb.2221930203

130. Jin J, Yoko T, Miyaji F, Sakka S, Fukunaga T, Misawa M. Neutron Diffraction Study on the Structure of Na-Si-O-N Oxynitride Glasses. *J Am Ceram Soc*. 1993;76(3):630–

634. https://doi.org/10.1111/j.1151-2916.1993.tb03652.x

131. Unuma H, Kawamura K, Sawaguchi N, Maekawa H, Yokokawa T. Molecular Dynamics Study of Na-Si-O-N Oxynitride Glasses. *J Am Ceram Soc*. 1993;76(5):1308–1312. https://doi.org/10.1111/j.1151-2916.1993.tb03756.x

132. Kohn S, Hoffbauer W, Jansen M, Franke R, Bender S. Evidence for the Formation of SiON Glasses. *J Non Cryst Solids*. 1998;224(3):232–243. https://doi.org/10.1016/S0022-3093(97)00467-5

133. Becher PF, Waters SB, Westmoreland CG, Riester L. Compositional Effects on the Properties of Si-Al-RE-Based Oxynitride Glasses (RE = La, Nd, Gd, Y, or Lu). *J Am Ceram Soc*. 2002;85(4):897–902. https://doi.org/10.1111/j.1151-2916.2002.tb00189.x

134. Hampshire S, Pomeroy MJ. Oxynitride Glasses. *Int J Appl Ceram Technol*. 2008;5(2):155–163. https://doi.org/10.1111/j.1744-7402.2008.02205.x

135. Larson RW, Day DE. Preparation and Characterization of Lithium Phosphorus Oxynitride Glass. *J Non Cryst Solids*. 1986;88(1):97–113. https://doi.org/10.1016/S0022-3093(86)80091-6

136. Pauthe M, Phalippou J, Belot V, Corriu R, Leclercq D, Vioux A. Preparation of Oxynitride Silicon Glass I. Nitridation of Hydrogenosilsesquioxane Xerogels. *J Non Cryst Solids*. 1990;125(3):187–194. https://doi.org/10.1016/0022-3093(90)90848-G

137. Leonova E, Hakeem AS, Jansson K, *et al.* Nitrogen-Rich La-Si-Al-O-N Oxynitride Glass Structures Probed by Solid State NMR. *J Non Cryst Solids*. 2008;354(1):49–60. https://doi.org/10.1016/j.jnoncrysol.2007.07.027

138. Koroglu A, Thompson DP, Apperley DC, Harris RK. Silicon/Aluminum and Oxygen/Nitrogen Ordering in Lanthanum U-Phase (La3Si3Al3O12N2). *J Solid State Chem*. 2004;177(8):2928–2932. https://doi.org/10.1016/j.jssc.2004.04.001

139. Dolekcekic E, Pomeroy MJ, Hampshire S. Structural Characterisation of Er-Si-Al-O-N

glasses by Raman Spectroscopy. *J Eur Ceram Soc*. 2007;27(2–3):893–898. https://doi.org/10.1016/j.jeurceramsoc.2006.04.058

140. Daucé R, Keding R, Sangleboeuf JC. On the Relations Between ISE and Structure in Some RE(Mg)SiAlO(N) Glasses. *J Mater Sci*. 2008;43(22):7239–7246. https://doi.org/10.1007/s10853-008-2851-3

141. Mascaraque N, Fierro JLG, Durán A, Muñoz F. An Interpretation for the Increase of Ionic Conductivity by Nitrogen Incorporation in LiPON Oxynitride Glasses. *Solid State Ionics*. 2013;233:73–79. https://doi.org/10.1016/j.ssi.2012.12.017

142. Mascaraque N, Durán A, Muñoz F, Tricot G. Structural Features of LiPON Glasses Determined by 1D and 2D 31P MAS NMR. *Int J Appl Glas Sci*. 2016;7(1):69–79. https://doi.org/10.1111/ijag.12120

143. Muñoz F, Delevoye L, Montagne L, Charpentier T. New Insights Into the Structure of Oxynitride NaPON Phosphate Glasses by 17-Oxygen NMR. *J Non Cryst Solids*. 2013;363(1):134–139. https://doi.org/10.1016/j.jnoncrysol.2012.12.028

144. Muñoz F, Pascual L, Durán A, Berjoan R, Marchand R. Validation of the Mechanism of Nitrogen/Oxygen Substitution in Li-Na-Pb-P-O-N Oxynitride Phosphate Glasses. *J Non Cryst Solids*. 2006;352(36–37):3947–3951. https://doi.org/10.1016/j.jnoncrysol.2006.06.016

145. Bunker BC, Tallant DR, Balfe CA, Kirkpatrick RJ, Turner GL, Reidmeyer MR. Structure of Phosphorus Oxynitride Glasses. *J Am Ceram Soc*. 1987;70(9):675–681. https://doi.org/10.1111/j.1151-2916.1987.tb05738.x

146. Sauze A Le, Montagne L, Palavit G, Fayon F, Marchand R. X-Ray Photoelectron Spectroscopy and Nuclear Magnetic Resonance Structural Study of Phosphorus Oxynitride Glasses, "LiNaPON." *J Non Cryst Solids*. 2000;263–264:139–145. https://doi.org/10.1016/s0022-3093(99)00630-4

147. Paraschiv GL, Muñoz F, Jensen LR, Yue Y, Smedskjaer MM. Impact of Nitridation of Metaphosphate Glasses on Liquid Fragility. *J Non Cryst Solids*. 2016;441:22–28. https://doi.org/10.1016/j.jnoncrysol.2016.03.009

148. Muñoz F, Pascual L, Durán A, Rocherullé J, Marchand R. Alkali and Alkali-Lead Oxynitride Phosphate Glasses: A Comparative Structural Study by NMR and XPS. *Comptes Rendus Chim*. 2002;5(11):731–738. https://doi.org/10.1016/S1631-0748(02)01434-0

149. Marchand R, Schnick W, Stock N. Molecular, Complex Ionic, and Solid State PON Compounds. *Adv Inorg Chem*. 2000;50:193–233. https://doi.org/10.1016/s0898-8838(00)50005-1

150. McMillan PF, Sato RK, Poe BT. Structural Characterization of Si-Al-O-N Glasses. *J Non Cryst Solids*. 1998;224(3):267–276. https://doi.org/10.1016/S0022-3093(97)00468-7

151. Nordmann A, Cheng YB, Smith ME. Role of Nitrides in Oxynitride Glasses and Glass-Ceramics: An NMR Investigation. *Chem Mater*. 1996;8(10):2516–2522. https://doi.org/10.1021/cm960238f

152. Sato RK, Bolvin J, McMillan PF. Synthesis and Characterization of a SiAlON Glass. *J Am Ceram Soc*. 1990;73(8):2494–2497. https://doi.org/10.1111/j.1151-2916.1990.tb07617.x

153. Luo Z, Lu A, Liu T, Song J, Han G. La2O3 Substitution in Li-Al-P-O-N Glasses for Potential Solid Electrolytes Applications. *Solid State Ionics*. 2016;295:104–110. https://doi.org/10.1016/j.ssi.2016.08.010

154. Mascaraque N, Tricot G, Revel B, Durán A, Muñoz F. Nitrogen and Fluorine Anionic Substitution in Lithium Phosphate Glasses. *Solid State Ionics*. 2014;254:40–47. https://doi.org/10.1016/j.ssi.2013.10.061

155. Brauer DS, Karpukhina N, Law R V., Hill RG. Structure of Fluoride-Containing Bioactive Glasses. *J Mater Chem*. 2009;19(31):5629–5636. https://doi.org/10.1039/b900956f

156. Schaller T, Dingwell DB, Keppler H, Knöller W, Merwin L, Sebald A. Fluorine in Silicate Glasses: A Multinuclear Nuclear Magnetic Resonance Study. *Geochim Cosmochim Acta*. 1992;56(2):701–707. https://doi.org/10.1016/0016-7037(92)90091-V

157. Stamboulis A, Hill RG, Law R V. Characterization of the Structure of Calcium Alumino-Silicate and Calcium Fluoro-Alumino-Silicate Glasses by Magic Angle Spinning Nuclear Magnetic Resonance (MAS-NMR). *J Non Cryst Solids*. 2004;333(1):101–107. https://doi.org/10.1016/j.jnoncrysol.2003.09.049

158. Mascaraque N, Takebe H, Tricot G, Fierro JLG, Durán A, Muñoz F. Structure and Electrical Properties of a New Thio-Phosphorus Oxynitride Glass Electrolyte. *J Non Cryst Solids*. 2014;405:159–162. https://doi.org/10.1016/j.jnoncrysol.2014.09.011

159. Mascaraque N, Fierro JLG, Muñoz F, *et al.* Thio-Oxynitride Phosphate Glass Electrolytes Prepared by Mechanical Milling. *J Mater Res*. 2015;30(19):2940–2948. https://doi.org/10.1557/jmr.2015.128

160. Kmiec S, Martin SW. Synthesis, Short-Range Order Structure, and Thermal Properties of Mixed Oxy-Sulfide Nitride (MOSN) Glasses. *Inorg Chem*. 2021;60(18):13968–13981. https://doi.org/10.1021/acs.inorgchem.1c00912

161. Ahmad S. Rare-Earth Aluminosilicate (RE2O3-Al2O3-SiO2) Glasses and Their Application as Solders for Joining of Silicon Carbide Components. *PhD Thesis, Fak für Maschinenbau*. 2017.

162. Rouxel T, Dély N, Sangleboeuf JC, *et al.* Structure-Property Correlations in Y-Ca-Mg-SiAlON Glasses: Physical and Mechanical Properties. *J Am Ceram Soc*. 2005;88(4):889–896. https://doi.org/10.1111/j.1551-2916.2005.00146.x

163. Videau JJ, Etourneau J, Garnier C, Verdier P, Laurent Y. Structural Influence of Nitrogen in Alkaline Earth Aluminosilicate Glasses: IR Absorption Spectroscopy. *Mater Sci Eng B*. 1992;15(3):249–254. https://doi.org/10.1016/0921-5107(92)90066-I

164. Thorp JS, Ahmad AB, Kulesza BLJ, Kenmuir SVJ. High-Frequency Dielectric Properties of Mg-Al-Si, Ca-Al-Si and Y-Al-Si Oxynitride Glasses. *J Mater Sci*. 1984;19:3211–3216. https://doi.org/10.1007/BF00549806

165. Kenmuir SVJ, Thorp JS, Kulesza BLJ. The Dielectric Behaviour of Mg-Al-Si, Ca-Al-Si, Y-Al-Si and Nd-Al-Si Oxynitride Glasses. *J Mater Sci*. 1983;18(6):1725–1730. https://doi.org/10.1007/BF00542068

166. Thorp JS, Kenmuir SVJ. Dielectric Properties of Some Oxynitride Glasses. *J Mater Sci*. 1981;16(5):1407–1409. https://doi.org/10.1007/BF01033858

167. Richet NF, Rouxel T, Kawaji H, Nicolas JM. Boson Peak, Elastic Properties, and Rigidification induced by the Substitution of Nitrogen for Oxygen in Oxynitride Glasses. *J Am Ceram Soc*. 2010;93(10):3214–3222. https://doi.org/10.1111/j.1551-2916.2010.03845.x

168. Rocherullé J, Matecki M, Delugeard Y. Heat Capacity Measurements of Mg-Y-Si-Al-O-N Glasses. *J Non Cryst Solids*. 1998;238(1–2):51–56. https://doi.org/10.1016/S0022-3093(98)00578-X

169. Rouxel T, Huger M, Besson JL. Rheological Properties of Y-Si-Al-O-N Glasses — Elastic Moduli, Viscosity and Creep. *J Mater Sci*. 1992;27(1):279–284. https://doi.org/10.1007/BF00553867

170. Holmes TM, Leatherman GL, El-Korchi T. Alkali-resistant oxynitride glasses. *J Mater Res*. 1991;6(1):152–158. https://doi.org/10.1557/JMR.1991.0152

171. Bachar A, Mercier C, Tricoteaux A, *et al.* Effects of Addition of Nitrogen on Bioglass Properties and Structure. *J Non Cryst Solids*. 2012;358(3):693–701.

https://doi.org/10.1016/j.jnoncrysol.2011.11.036

172. Le Sauze A, Gueguen E, Marchand R. Nitrided Glass as a Reaction Medium: Reduction of Ag and Cu within a Phosphorus Oxynitride Glass Matrix. *J Non Cryst Solids*. 1997;217(1):83–91. https://doi.org/10.1016/S0022-3093(97)00152-X

173. Le Sauze A, Gueguen E, Marchand R, Laurent Y. In-situ Precipitation of Metallic Silver and Copper within a Phosphorus Oxynitride Glass Matrix by Involving the N3-/N0 Redox Couple. *J Eur Ceram Soc*. 1997;17(15–16):1967–1970. https://doi.org/10.1016/s0955-2219(97)00066-6

174. Marchand R, Tessier F, Le Sauze A, Diot N. Typical Features of Nitrogen in Nitride-Type Compounds. *Int J Inorg Mater*. 2001;3(8):1143–1146. https://doi.org/10.1016/S1466-6049(01)00145-3

175. de Graaf D, Hintzen HT, Hampshire S, de With G. Long Wavelength Eu2+ Emission in Eu-Doped Y-Si-Al-O-N Glasses. *J Eur Ceram Soc*. 2003;23(7):1093–1097. https://doi.org/10.1016/S0955-2219(02)00236-4

176. De Graaf D, Hintzen HT, De With G. The Influence of the Composition on the Luminescence of Ce(III)-Ln-Si-Al-O-N Glasses (Ln = Sc, Y, La, Gd). *J Lumin*. 2003;104(1–2):131–136. https://doi.org/10.1016/S0022-2313(02)00688-9

177. Möncke D, Ali S, Jonson B, Kamitsos EI. Anion Polarizabilities in Oxynitride Glasses. Establishing a Common Optical Basicity Scale. *Phys Chem Chem Phys*. 2020;22(17):9543–9560. https://doi.org/10.1039/c9cp06930e

178. Kaplan-Diedrich H, Eckebracht A, Frischat GH. Viscosity and Surface Tension of Oxynitride Glass Melts. *J Am Ceram Soc*. 1995;78(4):1123–1124. https://doi.org/10.1111/j.1151-2916.1995.tb08454.x

179. Angell CA. Formation of Glasses from Liquids and Biopolymers. *Science*. 1995;267(5206):1924–1935. https://doi.org/10.1126/science.267.5206.1924

180. Reidmeyer MR, Rajaram M, Day DE. Preparation of Phosphorus Oxynitride Glasses. *J Non Cryst Solids*. 1986;85(1–2):186–203. https://doi.org/10.1016/0022-3093(86)90090-6

181. Makishima A, Mackenzie JD. Direct Calculation of Young's Modulus of Glass. *J Non Cryst Solids*. 1973;12(1):35–45. https://doi.org/10.1016/0022-3093(73)90053-7

182. Rocherulle J, Ecolivet C, Poulain M, Verdier P, Laurent Y. Elastic Moduli of Oxynitride Glasses. Extension of Makishima and Mackenzie's Theory. *J Non Cryst Solids*. 1989;108(2):187–193. https://doi.org/10.1016/0022-3093(89)90582-6

183. Daucé R, Verdier P, Laurent Y, Odriozola JA. An Approach to the Chemistry of Fracture in Oxynitride Glasses. *Ann Chim Sci des Mater*. 2003;28(2):79–86. https://doi.org/10.1016/S0151-9107(03)00035-7

184. Rouxel T, Yokoyama Y. Elastic Properties and Atomic Bonding Character in Metallic Glasses. *J Appl Phys*. 2015;118(4):044901. https://doi.org/10.1063/1.4926882

185. Paraschiv GL, Gomez S, Mauro JC, Wondraczek L, Yue Y, Smedskjaer MM. Hardness of Oxynitride Glasses: Topological Origin. *J Phys Chem B*. 2015;119(10):4109–4115. https://doi.org/10.1021/jp512235t

186. Rouxel T. Driving Force for Indentation Cracking in Glass: Composition, Pressure and Temperature Dependence. *Philos Trans R Soc A Math Phys Eng Sci*. 2015;373(2038):20140140. https://doi.org/10.1098/rsta.2014.0140

187. Diaz A, Hampshire S. Crystallisation of M-SiAlON Glasses to Iw-Phase Glass-Ceramics: Preparation and Characterisation. *J Mater Sci*. 2002;37(4):723–730. https://doi.org/10.1023/A:1013831612767

188. Sellappan P, Sharafat A, Keryvin V, *et al.* Elastic Properties and Surface Damage Resistance of Nitrogen-Rich (Ca,Sr)-Si-O-N Glasses. *J Non Cryst Solids*. 2010;356(41–42):2120–2126. https://doi.org/10.1016/j.jnoncrysol.2010.07.043

189. Bhatnagar A, Hoffman MJ, Dauskardt RH. Fracture and Subcritical Crack-Growth Behavior of Y-Si-Al-O-N Glasses and Si3N4 Ceramics. *J Am Ceram Soc*. 2000;83(3):585–596. https://doi.org/10.1111/j.1151-2916.2000.tb01237.x

190. Homeny J, Nelson GG, Paulik SW, Risbud SH. Comparison of the Properties of Oxycarbide and Oxynitride Glasses. *J Am Ceram Soc*. 1987;70(5):C-114-C-116. https://doi.org/10.1111/j.1151-2916.1987.tb05019.x

191. Luo Z, Han G, Lu A. Zn-Sr mixing in the Y-sialon glass: Formation, properties and ballistic resistance. *J Non Cryst Solids*. 2015;421:41–47. https://doi.org/10.1016/j.jnoncrysol.2015.04.035

192. Luo Z, Qu G, Zhang Y, Cui L, Lu A. Transparent oxynitride glasses: Synthesis, microstructure, optical transmittance and ballistic resistance. *J Non Cryst Solids*. 2013;378:45–49. https://doi.org/10.1016/j.jnoncrysol.2013.06.011

193. Bachar A, Mercier C, Tricoteaux A, Leriche A, Follet C, Hampshire S. Bioactive Oxynitride Glasses: Synthesis, Structure and Properties. *J Eur Ceram Soc*. 2016;36(12):2869–2881. https://doi.org/10.1016/j.jeurceramsoc.2015.12.017

194. Rouxel T. Fracture Surface Energy and Toughness of Inorganic Glasses. *Scr Mater*. 2017;137:109–113. https://doi.org/10.1016/j.scriptamat.2017.05.005

195. To T, Célarié F, Gueguen Y, *et al.* Environment Dependence of KIc of Glass. *J Non Cryst Solids*. 2021;566:120873. https://doi.org/10.1016/j.jnoncrysol.2021.120873

196. Tajima Y, Urashima K. Tailoring of Mechanical Properties of Si3N4 Ceramics. Ed. by M. J. Hoffmann and G. Petzow, Kluwer, Dordrecht, Netherlands; 1994

197. Reimanis IE, Suematsu H, Petrovic JJ, Mitchell TE. Mechanical Properties of Single-Crystal α-Si3N4. *J Am Ceram Soc*. 1996;79(8):2065–2073. https://doi.org/10.1111/j.1151-2916.1996.tb08938.x

198. Coon DN. Subcritical Crack Growth in Y-Al-Si-O-N Glass. *J Non Cryst Solids*.

1998;226(3):281–286. https://doi.org/10.1016/S0022-3093(98)00454-2

199. Rouxel T. Thermodynamics of Viscous Flow and Elasticity of Glass Forming Liquids in the Glass Transition Range. *J Chem Phys*. 2011;135(18):184501. https://doi.org/10.1063/1.3656695

200. Angell CA. Perspective on the Glass Transition. *J Phys Chem Solids*. 1988;49(8):863–871. https://doi.org/10.1016/0022-3697(88)90002-9

201. Rouxel T, Sanglebœuf JC, Huger M, Gault C, Besson JL, Testu S. Temperature Dependence of Young's Modulus in Si3N4-based Ceramics: Roles of Sintering Additives and of SiC-Particle Content. *Acta Mater*. 2002;50(7):1669–1682. https://doi.org/10.1016/S1359-6454(02)00004-6

202. Gueguen Y, Sharafat A, Grins J, Rouxel T. Viscosity of High-Nitrogen Content Ca-Si-O-N Glasses. *J Eur Ceram Soc*. 2010;30(16):3455–3458. https://doi.org/10.1016/j.jeurceramsoc.2010.07.039

203. Unuma H, Kokubo T, Sakka S. Crystallization of Li-Si-O-N Oxynitride Glasses. *J Mater Sci*. 1988;23(12):4399–4405. https://doi.org/10.1007/BF00551938

204. Rocherullé J. Determination of the Nucleation Rate Type Curves of a LAS Oxynitride Glass. *J Mater Sci Lett*. 2003;22(13):923–925. https://doi.org/10.1023/A:1024614118124

205. Singh SP, Rodrigues AM, Orsolini HD, *et al.* Crystallization Pathways and Some Properties of Lithium Disilicate Oxynitride Glasses. *Ceram Int*. 2017;43(15):12348–12356. https://doi.org/10.1016/j.ceramint.2017.06.100

206. Deckwerth M, Rüssel C. Crystallization of Oxynitride Glasses in the System Mg-Ca-Al-Si-O-N Prepared with the Aid of a Polymeric Precursor. *J Non Cryst Solids*. 1997;217(1):55–65. https://doi.org/10.1016/S0022-3093(97)00149-X

207. Höche T, Deckwerth M, Rüssel C. Partial Stabilization of Tetragonal Zirconia in

Oxynitride Glass-Ceramics. *J Am Ceram Soc*. 1998;81(8):2029–2036. https://doi.org/10.1111/j.1151-2916.1998.tb02584.x

208. Menke Y, Hampshire S, Falk LKL. Effect of Composition on Crystallization of Y/Yb-Si-Al-O-N B-Phase Glasses. *J Am Ceram Soc*. 2007;90(5):1566–1573. https://doi.org/10.1111/j.1551-2916.2007.01580.x

209. Luo Z, Lu A, Hu X, Liu W. Effects of Nitrogen on Phase Formation, Microstructure and Mechanical Properties of Y-Ca-Si-Al-O-N Oxynitride Glass-Ceramics. *J Non Cryst Solids*. 2013;368(1):79–85. https://doi.org/10.1016/j.jnoncrysol.2013.03.005

210. Sebaï M, Penot C, Goursat P, *et al.* Oxidation Resistance of Nd-Si-Al-O-N Glasses and Glass-Ceramics. *J Eur Ceram Soc*. 1998;18(2):169–182. https://doi.org/10.1016/S0955-2219(97)00090-3

211. Unuma H, Miura K, Furusaki T, Kodaira K. Preparation and Properties of Glass-Ceramics Derived from Nitrogen-Containing β-Spodumene Glasses. 2000;95(197214):1291–1295. https://doi.org/10.1111/j.1151-2916.1991.tb04100.x

212. Lederer K, Deckwerth M, Rüssel C. Zirconia-Doped Mg-Ca-Al-Si-O-N Glasses: Crystallization. *J Non Cryst Solids*. 1998;224(2):109–121. https://doi.org/10.1016/S0022-3093(97)00441-9

213. Qu G, Luo Z, Liu W, Lu A. The Preparation and Properties of Zirconia-Doped Y-Si-Al-O-N Oxynitride Glasses and Glass-Ceramics. *Ceram Int*. 2013;39(8):8885–8892. https://doi.org/10.1016/j.ceramint.2013.04.082

214. Baron B, Chartier T, Rouxel T, Verdier P, Laurent Y. SiC Particle Reinforced Oxynitride Glass: Processing and Mechanical Properties. *J Eur Ceram Soc*. 1997;17:773–780. https://doi.org/10.1016/S0955-2219(96)00165-3

215. Rouxel T, Lavelle C, Garnier C, Verdier P, Laurent Y. Mechanical Evaluation of SiC Particle Reinforced Oxynitride Glass and Glass-Ceramic Composites. *Scr Metall*

Mater. 1994;31(I):15–20. https://doi.org/10.1016/0956-716X(94)90087-6

216. Zhang E, Thompson DP, Gao L. Interfacial Characterization of Nicalon SiC Fibre Reinforced Oxynitride Glass Matrix Composites. *J Mater Sci*. 1997;32(17):4501–4506. https://doi.org/10.1023/A:1018660915306

217. Iba H, Chang T, Kagawa Y, Minakuchi H, Kanamaru K. Fabrication of optically transparent short-fiber-reinforced glass matrix composites. *J Am Ceram Soc*. 1996;79(4):881–884. https://doi.org/10.1111/j.1151-2916.1996.tb08520.x

218. Suganuma K, Minakuchi H, Kada K, Kitamura T, Osafune H, Fujii H. Properties and microstructure of continuous oxynitride glass fiber and its application to aluminum matrix composite. *J Mater Res*. 1993;8(1):178–186. https://doi.org/10.1557/JMR.1993.0178

219. Satet RL, Hoffmann MJ, Cannon RM. Experimental Evidence of the Impact of Rare-Earth Elements on Particle Growth and Mechanical Behaviour of Silicon Nitride. *Mater Sci Eng A*. 2006;422(1–2):66–76. https://doi.org/10.1016/j.msea.2006.01.015

220. Kramer M, Hoffmann MJ, Petzow G. Grain Growth Kinetics of Si3N4 During α/β-Transformation. *Acta Metall Mater*. 1993;41(10):2939–2947. https://doi.org/10.1016/0956-7151(93)90108-5

221. Sun EY, Becher PF, Hsueh CH, *et al.* Debonding Behavior Between β-Si3N4 Whiskers and Oxynitride Glasses with or without an Epitaxial β-SiAlON Interfacial Layer. *Acta Mater*. 1999;47(9):2777–2785. https://doi.org/10.1016/S1359-6454(99)00122-6

222. Machacek J, Gedeon O, Liska M, Charvatova S. First Principles Molecular Dynamics of Silicate Oxynitride Melt Doped with Scandium, Yttrium and Lanthanum. *J Non Cryst Solids*. 2007;353(18–21):2025–2028. https://doi.org/10.1016/j.jnoncrysol.2007.01.067

223. Murakami M, Sakka S. Ab initio Molecular Rrbital Calculation of the Interatomic

Potential and Force Constants in Silicon Oxynitride Glass. *J Non Cryst Solids*. 1988;101(2–3):271–279. https://doi.org/10.1016/0022-3093(88)90163-9

224. Allison T. JANAF Thermochemical Tables, NIST Standard Reference Database 13. National Institute of Standards and Technology; 1996 https://doi.org/10.18434/T42S31

225. Reed JJ. The NBS Tables of Chemical Thermodynamic Properties: Selected Values for Inorganic and C1 and C2 Organic Substances in SI Units. National Institute of Standards and Technology; 2020 https://doi.org/10.18434/M32124

226. Dériano S. Conception Chimique de Verres Silicatés à Hautes Performances Mécaniques. *PhD Thesis, Univ Rennes 1*. 2002.

227. Ecolivet C, Verdier P. Propriétés Elastiques et Indices de Réfraction de Verres Azotés. *Mater Res Bull*. 1984;19:227–231.

228. Schrimpf C, Frischat GH. Property-Composition Relations of N2-Containing Na2O-CaO-SiO2 Glasses. *J Non Cryst Solids*. 1983;56(1–3):153–159. https://doi.org/10.1016/0022-3093(83)90461-1

229. Tsukuma K, Akiyama T. High Temperature Viscosity of Nitrogen Modified Silica Glass. *J Non Cryst Solids*. 2000;265(3):199–209. https://doi.org/10.1016/S0022-3093(00)00005-3

230. Lemercier H, Rouxel T, Fargeot D, Besson JL, Piriou B. Yttrium SiAlON Glasses: Structure and Mechanical Properties - Elasticity and Viscosity. *J Non Cryst Solids*. 1996;201(1–2):128–145. https://doi.org/10.1016/0022-3093(96)00147-0

231. Drew RAL, Hampshire S, Jack KH. Nitrogen Glasses. 1981;31(in: P. Popper, D.E. Taylor (Eds.), Brit. Cer. Pr.):119–132.

TABLE I. High temperature elastic properties of a SiYAlON oxynitride glasses with 17 e/o N (adapted from [23] and [199]). Typical glasses from other chemical systems are also reported for comparison. [1)]From Dilatometry or Differential Scanning Calorimetry; [2)]Transition temperature observed in the $\mu(T)$ measurements by means of ultrasonic echography. [3)]Softening rates measured in the glassy (-) and in the supercooled-liquid (+) range near T_g. [4)]α as obtained by smoothly fitting the experimental data in the supercooled liquid range.

Glass	T_g[1)] (K)	T_g[2)] (K)	E_{RT} (GPa)	μ_{RT} (GPa)	$\mu(T_g)$ (GPa)	$E(T_g)$ (GPa)	$d\mu/dT$ (T_g^-)[3)] (MPa·K^{-1})	dE/dT (T_g^-)[3)] (MPa·K^{-1})	$d\mu/dT$ (T_g^+)[3)] (MPa·K^{-1})	α[4)]
a-SiO_2	1463	1370	70	30.4	31	76.8	3.14	2.95	-5.30	0.07
$Y_{12.3}Si_{18.5}Al_7O_{54.7}N_{7.5}$	1216	1236	142	55	45.2	122	-8.53	-103	-247	9.0
$Zr_{55}Cu_{30}Al_{10}Ni_5$	683	651	81	29.5	27.4	72.9	-2.37	-108	-31.3	0.78
Soda-lime-silica	835	823	72	29.3	27.1	56	-4.74	-67	-30.9	0.98
Glycerol	193	193	1.03	0.35	4.8	9.5	-22.5	-190	-28.8	1.26

TABLE II. Viscous flow properties of an oxynitride glass with 17 e/o N in the transition range (reprinted from [199]). [1)]Glass transition temperature taken as the temperature at which $\eta = 10^{12}$ Pa·s; [2)]Viscosity at T_g as determined by *DSC*; [3)]As defined by $m = d\log_{10}\eta / d(T(\eta = 10^{12}$ Pa·s)/T);

Glass	T_g[1)] (K)	$\eta(T_g)$[2)] x10^{12} Pa·s	$\Delta H_a(T_g)$ (kJ·mol^{-1})	$\Delta S_a(T_g)$ (J·K^{-1}·mol^{-1})	m[3)]
a-SiO_2	1463	0.8	510	66	18
$Y_{12.3}Si_{18.5}Al_7O_{54.7}N_{7.5}$	1216	1.9	1115	799	48
$Zr_{55}Cu_{30}Al_{10}Ni_5$	683	8	428	267	33
Soda-lime-silica	835	3	571	331	36
Glycerol	193	3	253	704	68

FIGURE CAPTIONS

FIGURE 1 Number of papers focusing on bulk oxynitride glasses per country before 2010 (red), and during the last 10 years (blue).

FIGURE 2 The glass forming region in the Y-Si-Al-O-N system at 1700 °C extending up to about 7 at.% N, or 25 e/o N (reprinted from [231]).

FIGURE 3 Photographs of 4 mm thick glass specimens in the SiO_2-BaO-Al_2O_3-Si_3N_4 system with 0 to 27 e/o N.

FIGURE 4 Schematic drawing and pictures of the atmosphere-controlled melting, quenching and annealing facilities at the Glass Mechanics Lab. (Rennes, France).

FIGURE 5 Gibbs free energies of various $\frac{2}{y} M + O_2 = \frac{2}{y} MO_y$ and $\frac{2}{y} AN_x + O_2 = \frac{2}{y} AO_y + \frac{x}{y} N_2$ reactions with increasing temperature, normalized to 1 mole O_2 [224] [225]. When a nitride can be oxidized into various oxide species (like VO, V_2O_3, VO_2 or V_2O_5 in the case of vanadium), only the reaction showing the lowest Gibbs free energies in the temperature range is shown (as it is the one that will reduce the most oxides).

FIGURE 6 The substitution of oxygen by nitrogen with the formation of 2-fold and 3-fold coordinated nitrogen atoms in phosphate oxynitride glasses [46].

FIGURE 7 Preferential substitution of oxygen bridging PO_4-PO_3N tetrahedra [146].

FIGURE 8 Dissociation energy $< U_0 >$ as a function of the glass transition temperature (T_g) for glasses from different chemical systems (elemental symbols represent host elements of metallic glasses). Reprinted with some modification from ref. [184].

FIGURE 9 Bulk modulus (experiments) as a function of the glass transition temperature (reprinted and adapted from ref. [23]).

FIGURE 10 Poisson's ratio, ν, as a function of the atomic packing density, C_g (reprinted and adapted from ref. [23]).

FIGURE 11 Young's modulus of oxynitride glasses with increasing nitrogen content [226] [227] [126] [228] [229].

FIGURE 12 Bulk modulus, K, as a function of the volume density of energy $< U_0 > / < V_0 >$ [230] [169] [226] [162] [227] [228] [188].

FIGURE 13 Hardness (mostly from Vickers indentation tests) as a function of the glass transition temperature (reprinted and adapted from ref. [23]).

FIGURE 14 Hardness of silicon oxynitride glasses as a function of the nitrogen content in eq. % N. Reprinted with permission from [185].

FIGURE 15 Indentation cracking and driving-force map. Stress components are taken at the border of the indentation imprint for sake of simplicity. Recall that $\sigma_{rr}(\theta=\pi/2)$, $\sigma_{\phi\phi}(\theta=\pi/2)$, $\sigma_{rr}(\theta=0)$, $\sigma_{\theta\theta}(\theta=0)$ are the stress components governing the ring/cone-, the radial-, the subsurface lateral-, and the median-cracks respectively (spherical coordinates with $\theta=0$ for the

vertical axis). (-) and (+) signs indicate the area where the stress component is compressive and tensile respectively. The red contour shows where the driving force is expected to vanish. Reprinted and adapted with permission from ref. [186]. The inset shows the radial cracks at a Vickers indentation site (4.9 N applied for 15 s) on a $Sr_{12.73}Si_{10}O_{20.08}N_{8.44}$ oxynitride glass (the bar is equal to 50 μm) [188].

FIGURE 16 Measured and calculated fracture toughness of various oxynitride glasses [187 188 65 189 190 191 192 193]. Round dots indicate fracture toughness measured by chevron notched specimen technique, and squared dots indicate fracture toughness measured by indentation or other techniques.

FIGURE 17 Temperature dependence of Young's modulus of glasses from different chemical systems (reprinted and adapted with permission from ref. [23].

FIGURE 18 Temperature dependence of shear modulus (μ). The curve fitting at $T > T_g$ corresponds to $\mu / \mu(T_g) = (T_g / T)^{\alpha}$ (reprinted and adapted from ref. [199]).

FIGURE 19 Shear viscosity coefficient, η, of glasses from different chemical system.

FIGURE 20 T_g-scaled logarithm of the shear viscosity coefficient (η) in the transition range from which the activation energy for flow as well as the fragility index are straightforwardly derived from the slope of the linear intercepts (reprinted and adapted from ref. [199]).

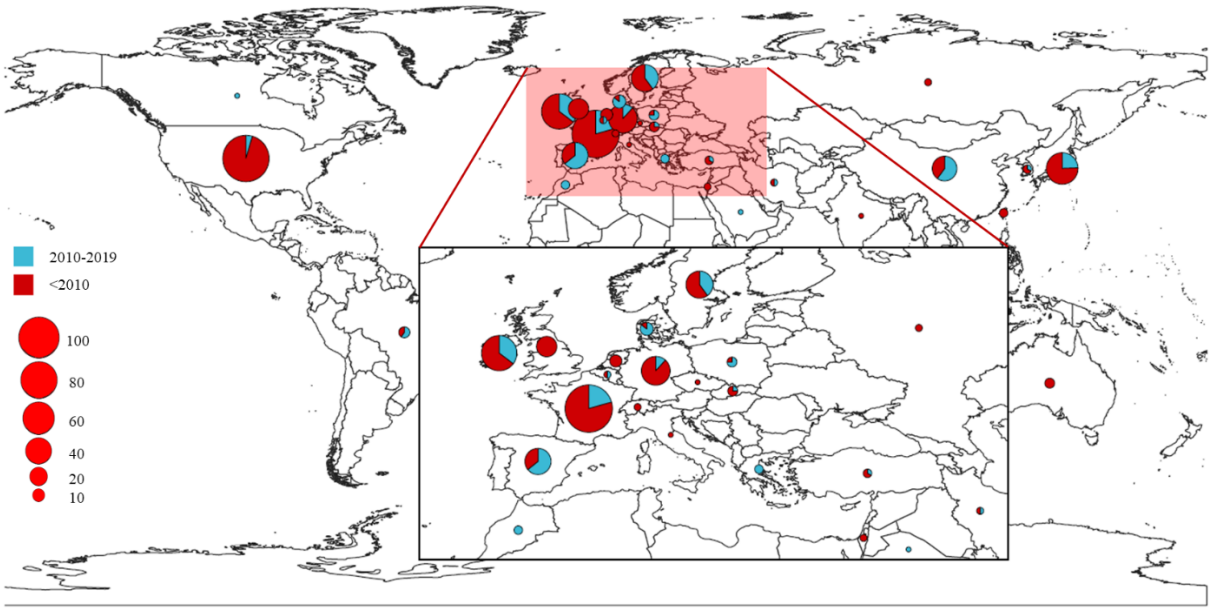

FIGURE 1 Number of papers focusing on bulk oxynitride glasses per country before 2010 (red), and during the last 10 years (blue).

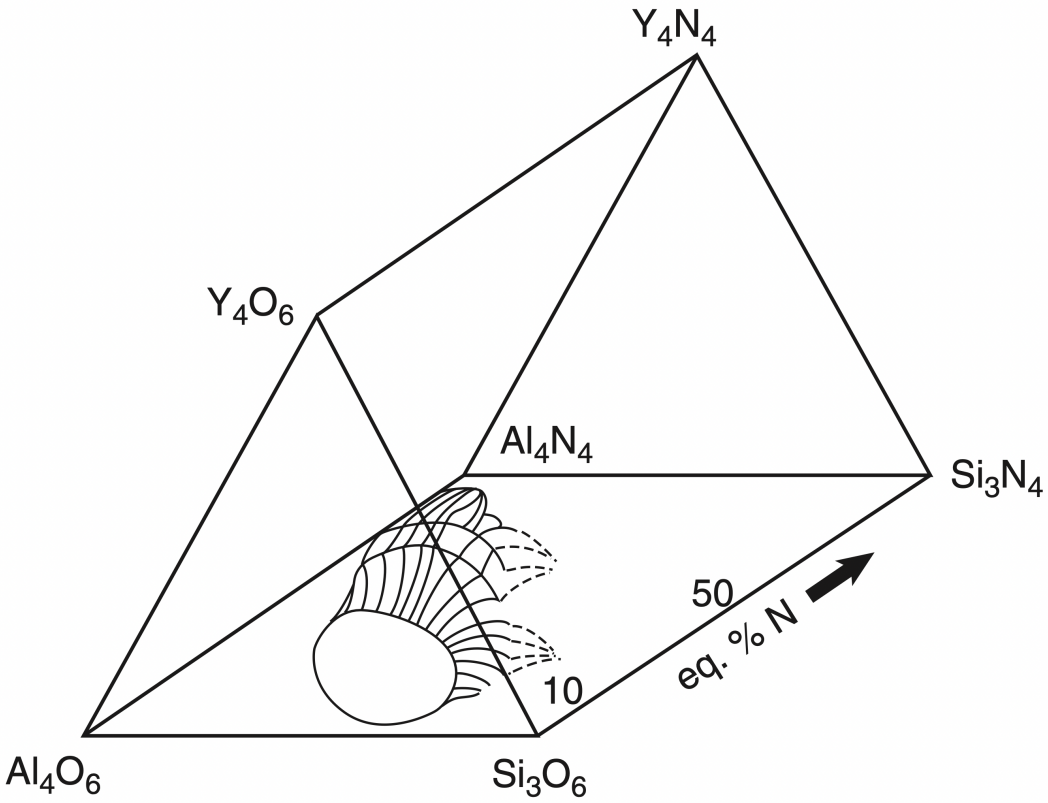

FIGURE 2 The glass forming region in the Y-Si-Al-O-N system at 1700 °C extending up to about 7 at.% N, or 25 e/o N (reprinted from [231]).

FIGURE 3 Photographs of 4 mm thick glass specimens in the SiO_2-BaO-Al_2O_3-Si_3N_4 system with 0 to 27 e/o N.

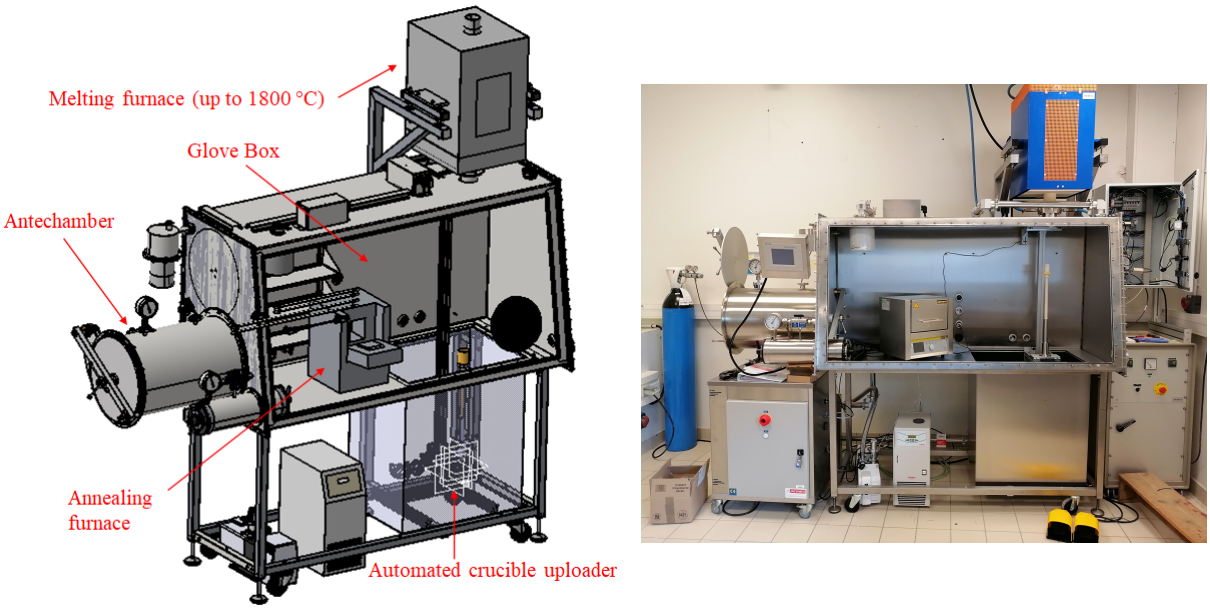

FIGURE 4 Schematic drawing and pictures of the atmosphere-controlled melting, quenching and annealing facilities at the Glass Mechanics Lab. (Rennes, France).

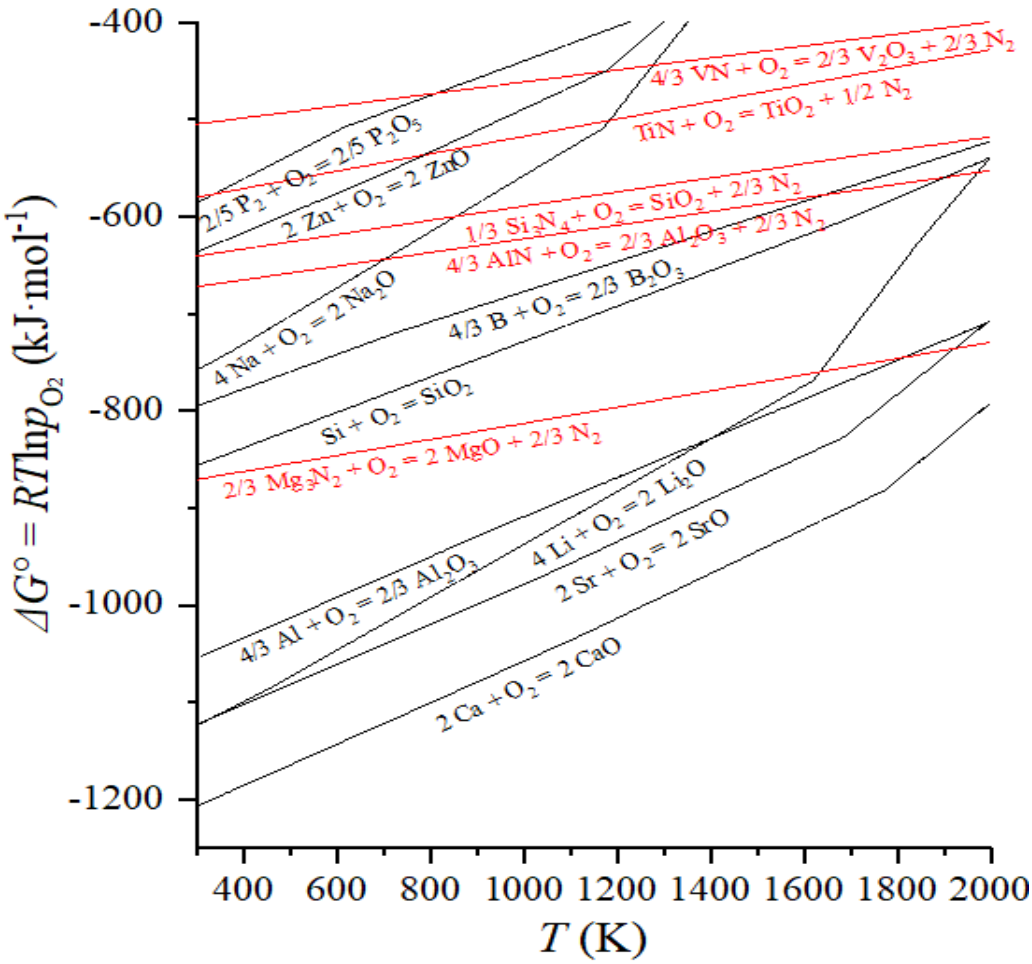

FIGURE 5 Gibbs free energies of various $\frac{2}{y}M + O_2 = \frac{2}{y}MO_y$ and $\frac{2}{y}AN_x + O_2 = \frac{2}{y}AO_y + \frac{x}{y}N_2$ reactions with increasing temperature, normalized to 1 mole O_2 [224] [225]. When a nitride can be oxidized into various oxide species (like VO, V_2O_3, VO_2 or V_2O_5 in the case of vanadium), only the reaction showing the lowest Gibbs free energies in the temperature range is shown (as it is the one that will reduce the most oxides).

1605

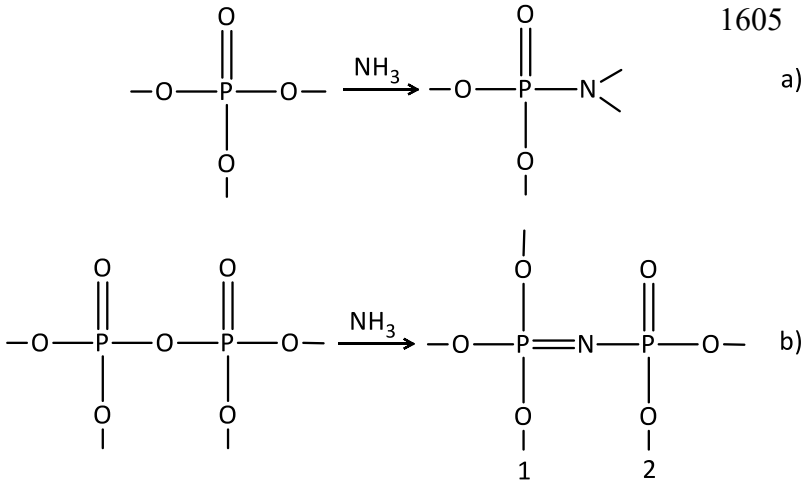

FIGURE 6 The substitution of oxygen by nitrogen with the formation of 2-fold and 3-fold coordinated nitrogen atoms in phosphate oxynitride glasses [46].

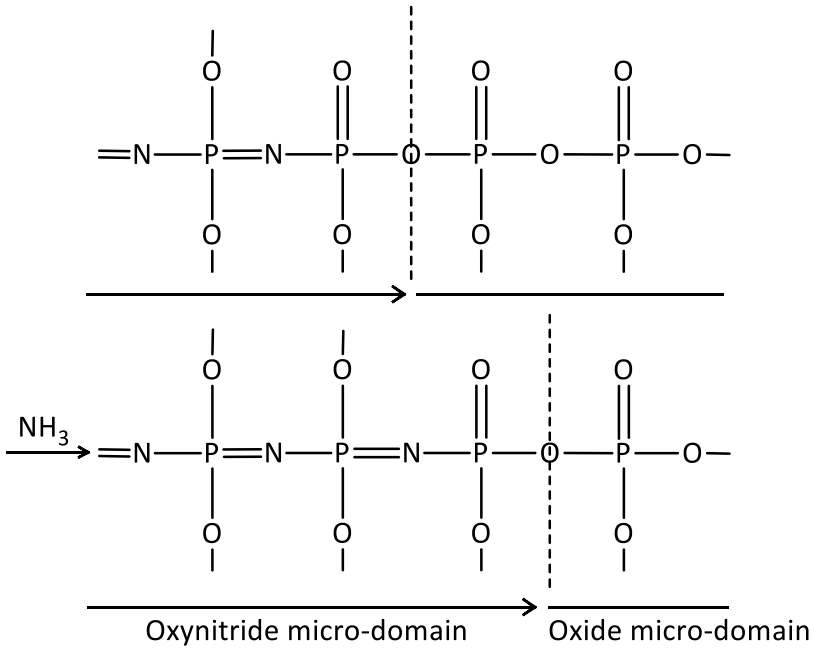

FIGURE 7 Preferential substitution of oxygen bridging PO_4-PO_3N tetrahedra [146].

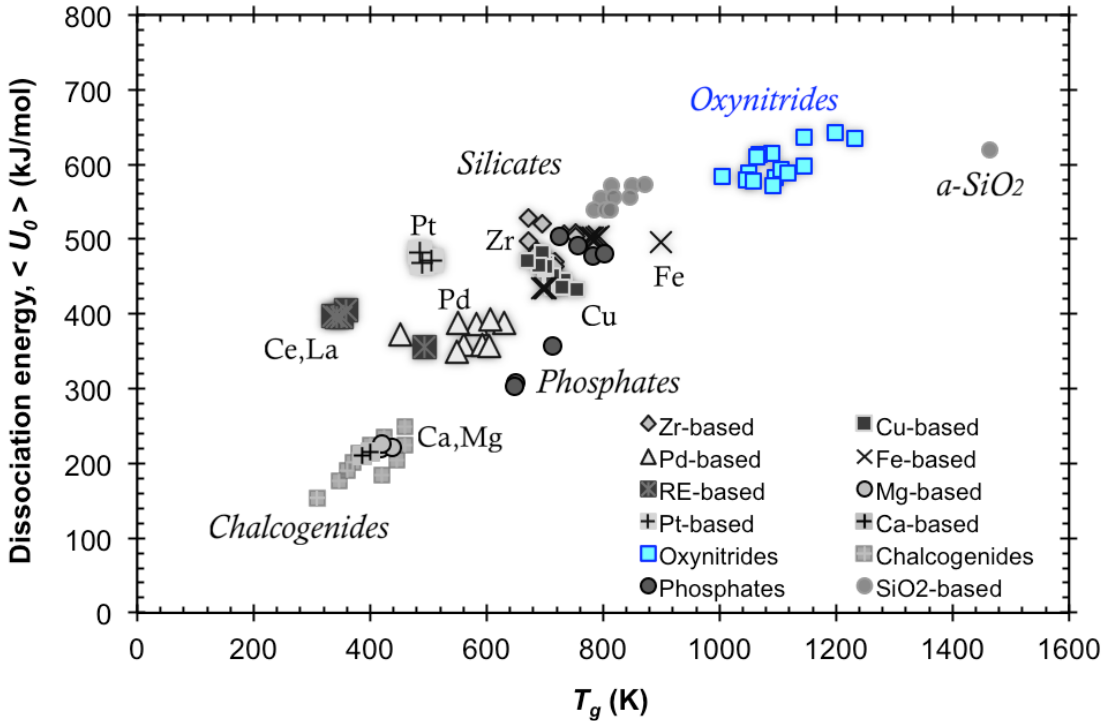

FIGURE 8 Dissociation energy $< U_0 >$ as a function of the glass transition temperature (T_g) for glasses from different chemical systems (elemental symbols represent host elements of metallic glasses). Reprinted with some modification from ref. [184].

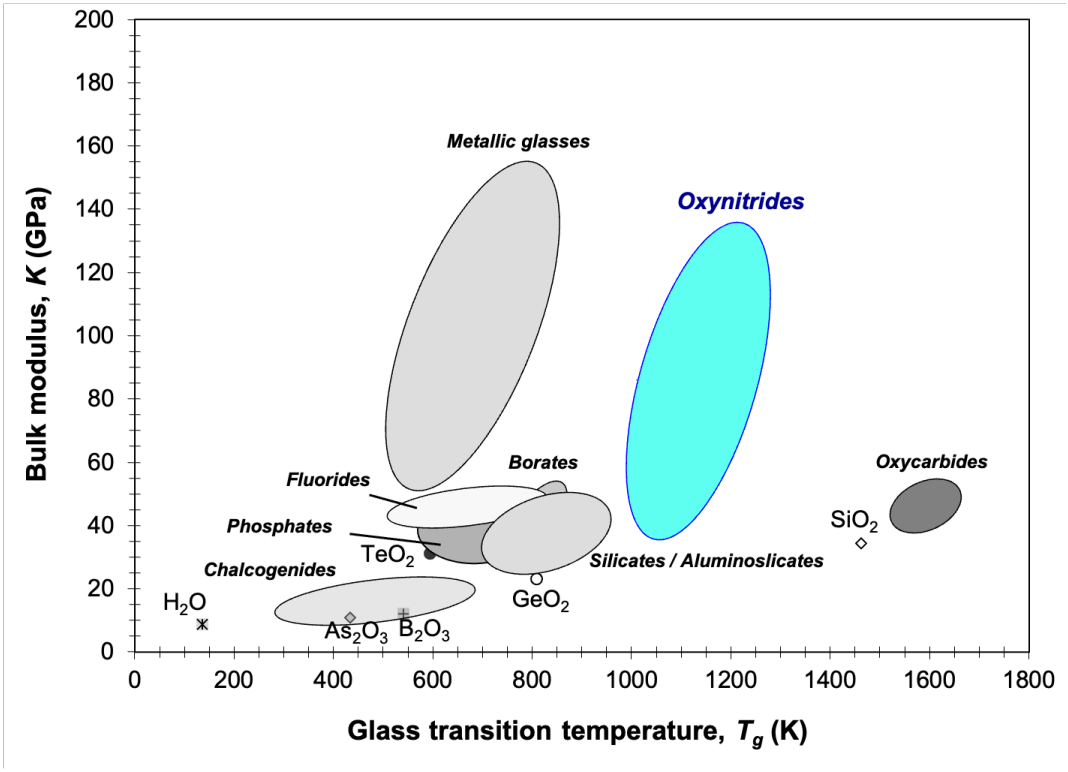

FIGURE 9 Bulk modulus (experiments) as a function of the glass transition temperature (reprinted and adapted from ref. [23]).

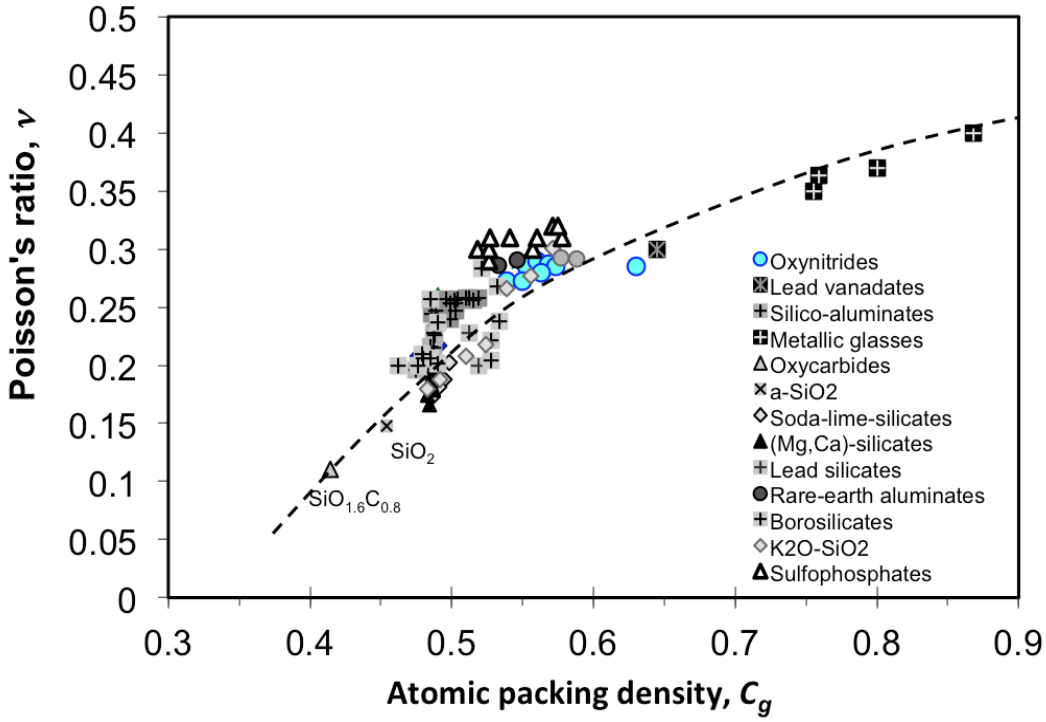

FIGURE 10 Poisson's ratio, ν, as a function of the atomic packing density, C_g (reprinted and adapted from ref. [23]).

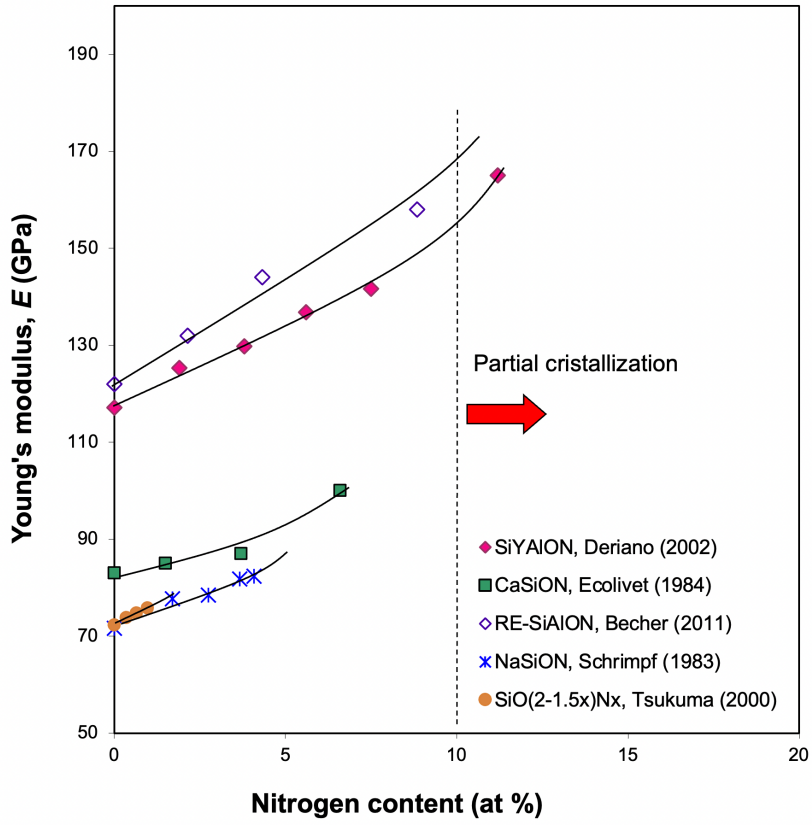

1637

1638 **FIGURE 11** Young's modulus of oxynitride glasses with increasing nitrogen content
1639 [226 227 126 228 229].

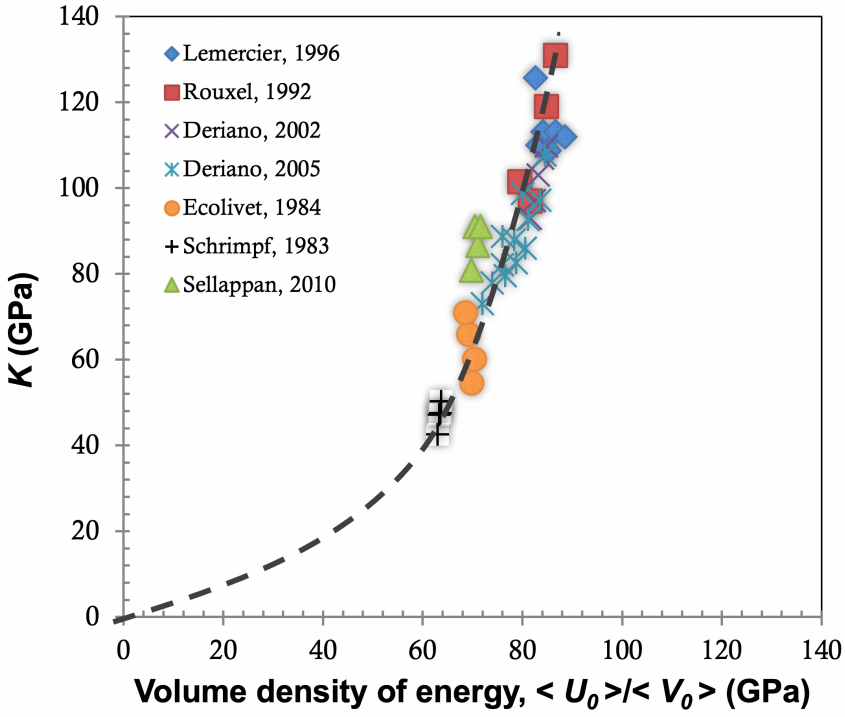

1640

1641

1642 **FIGURE 12** Bulk modulus, K, as a function of the volume density of energy $< U_0 >/< V_0 >$.
1643 Data from refs. [230 169 226 162 227 228 188].

1644

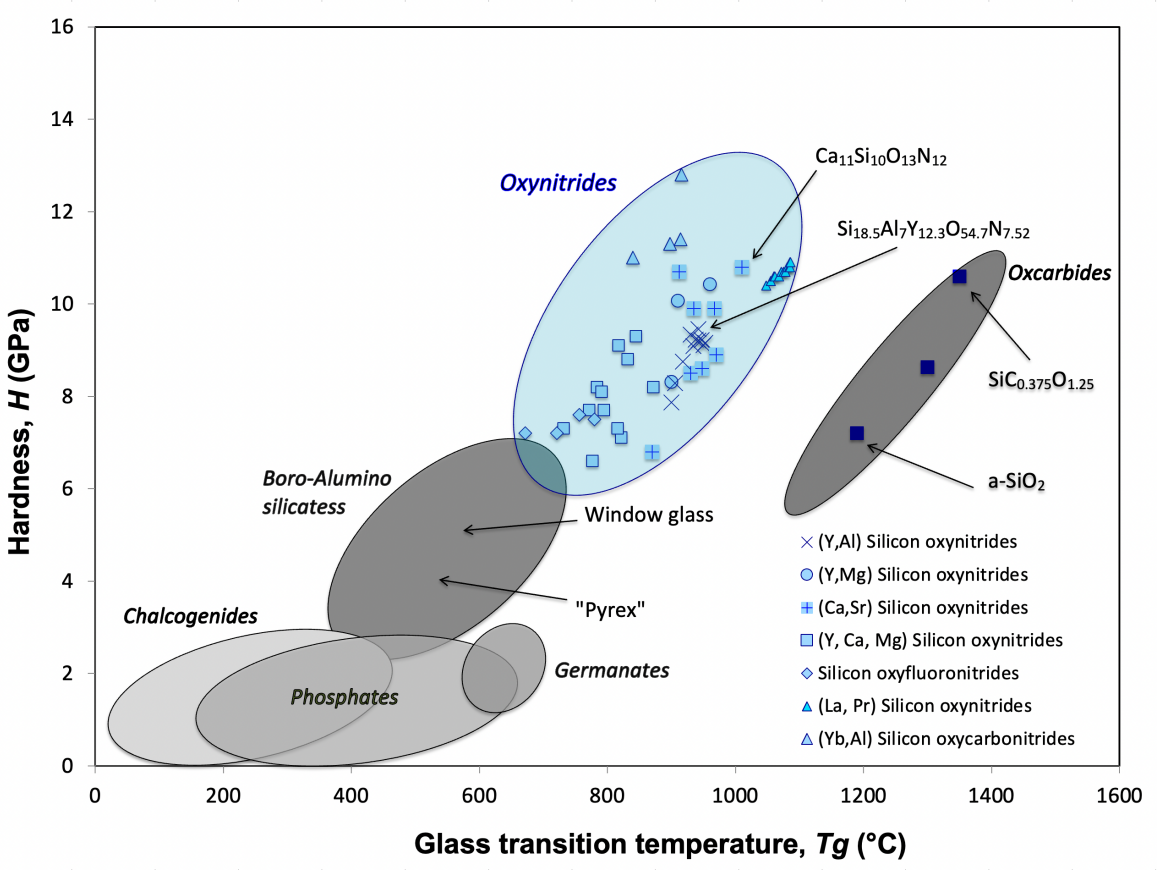

1645

1646 **FIGURE 13** Hardness (mostly from Vickers indentation tests) as a function of the glass
1647 transition temperature (reprinted and adapted from ref. [23]).

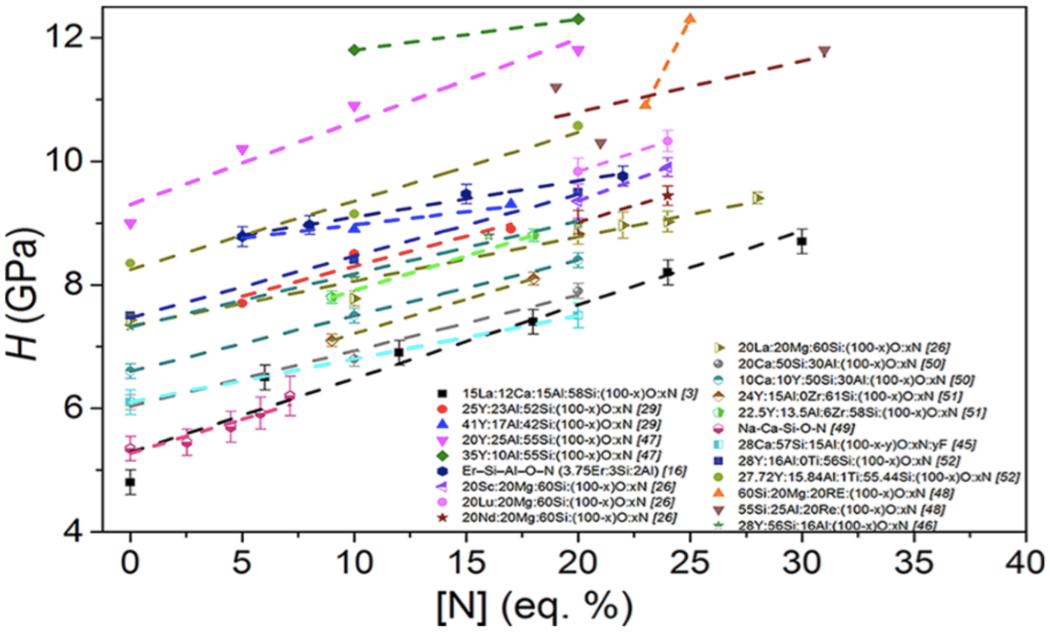

1648

1649 **FIGURE 14** Hardness of silicon oxynitride glasses as a function of the nitrogen content in eq.
1650 % N. Reprinted with permission from [185].

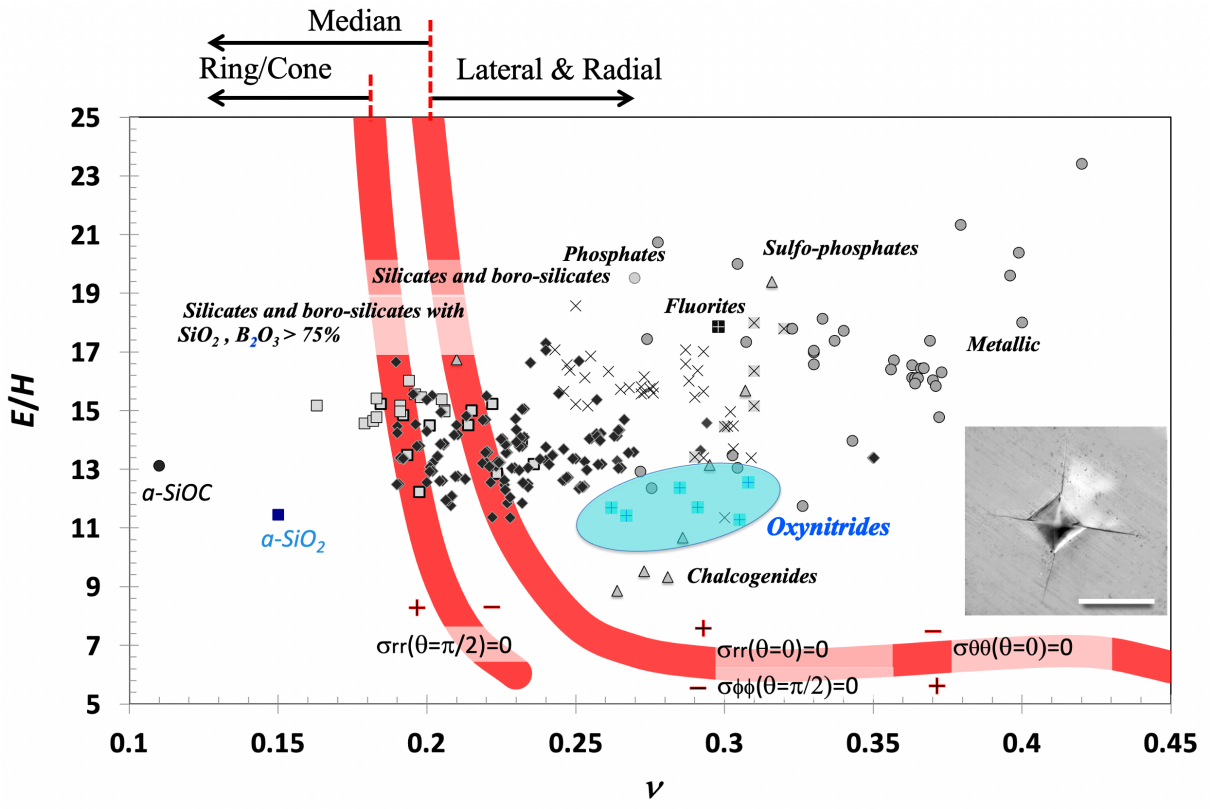

FIGURE 15 Indentation cracking and driving-force map. Stress components are taken at the border of the indentation imprint for sake of simplicity. Recall that $\sigma_{rr}(\theta=\pi/2)$, $\sigma_{\phi\phi}(\theta=\pi/2)$, $\sigma_{rr}(\theta=0)$, $\sigma_{\theta\theta}(\theta=0)$ are the stress components governing the ring/cone-, the radial-, the subsurface lateral-, and the median-cracks respectively (spherical coordinates with $\theta=0$ for the vertical axis). (-) and (+) signs indicate the area where the stress component is compressive and tensile respectively. The red contour shows where the driving force is expected to vanish. Reprinted and adapted with permission from ref. [186]. The inset shows the radial cracks at a Vickers indentation site (4.9 N applied for 15 s) on a $Sr_{12.73}Si_{10}O_{20.08}N_{8.44}$ oxynitride glass (the bar is equal to 50 μm) [188].

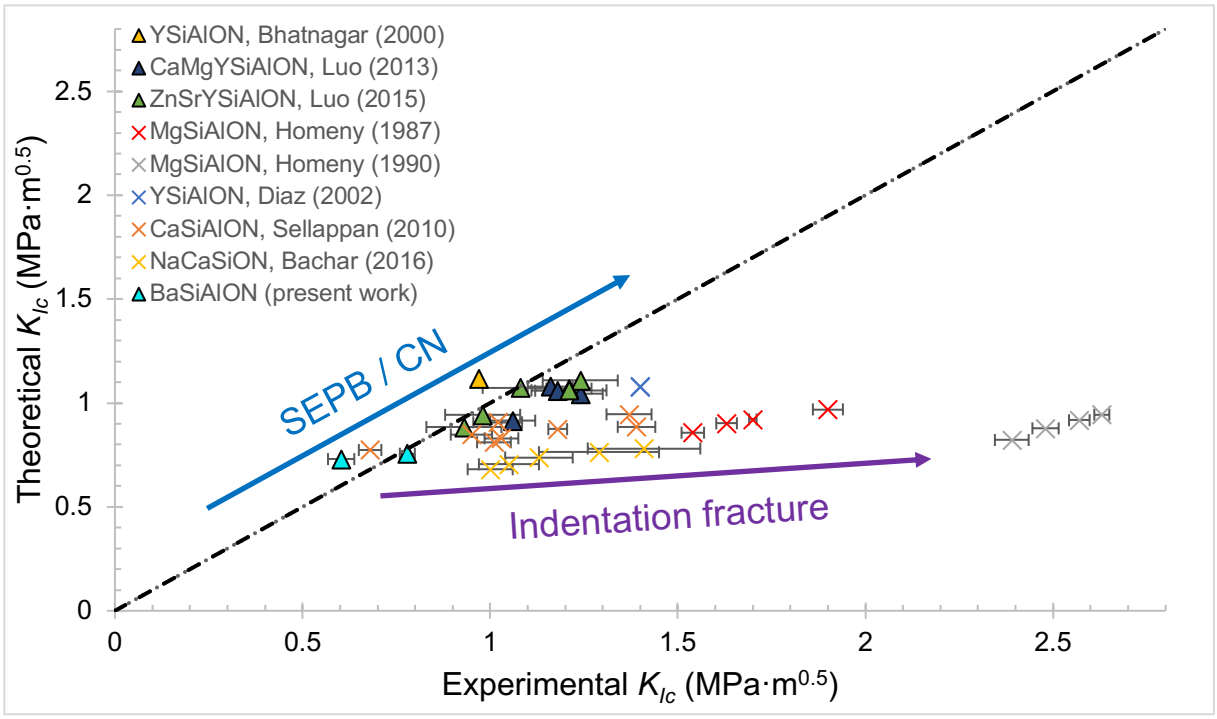

FIGURE 16 Measured and calculated fracture toughness of various oxynitride glasses [187 188 65 189 190 191 192 193]. Round dots indicate fracture toughness measured by chevron notched specimen technique, and squared dots indicate fracture toughness measured by indentation or other techniques.

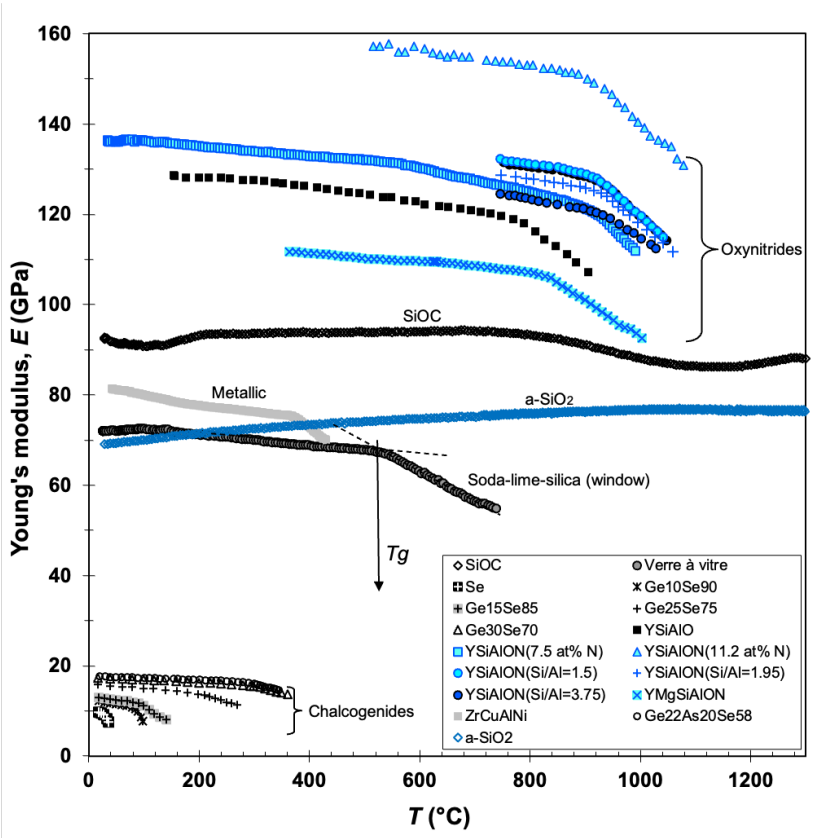

FIGURE 17 Temperature dependence of Young's modulus of glasses from different chemical systems (reprinted and adapted with permission from ref. [23]).

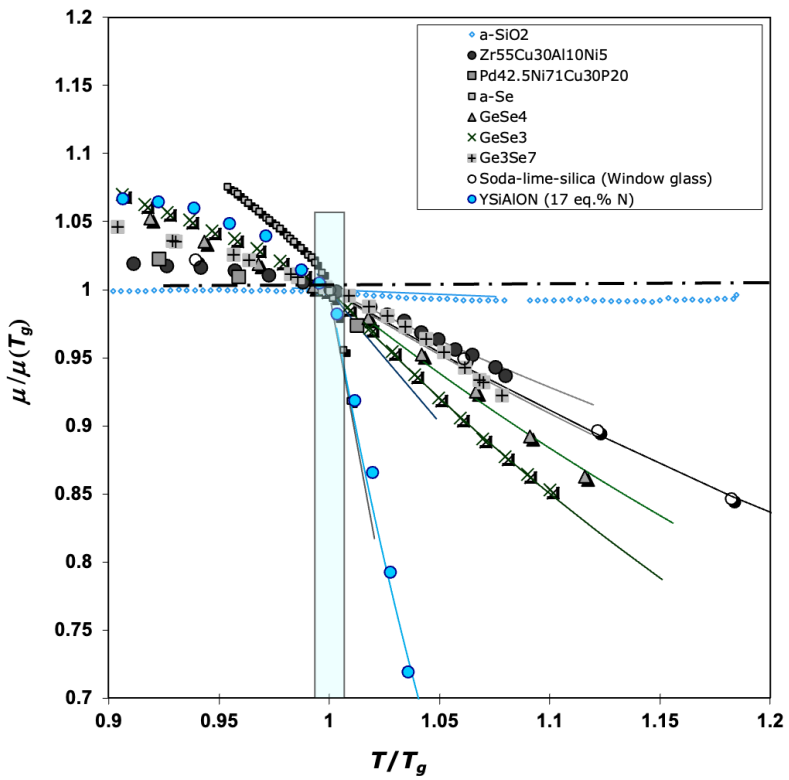

FIGURE 18 Temperature dependence of shear modulus (μ). The curve fitting at $T > T_g$ corresponds to $\mu/\mu(T_g) = (T_g/T)^{\alpha}$ (reprinted and adapted from ref. [199]).

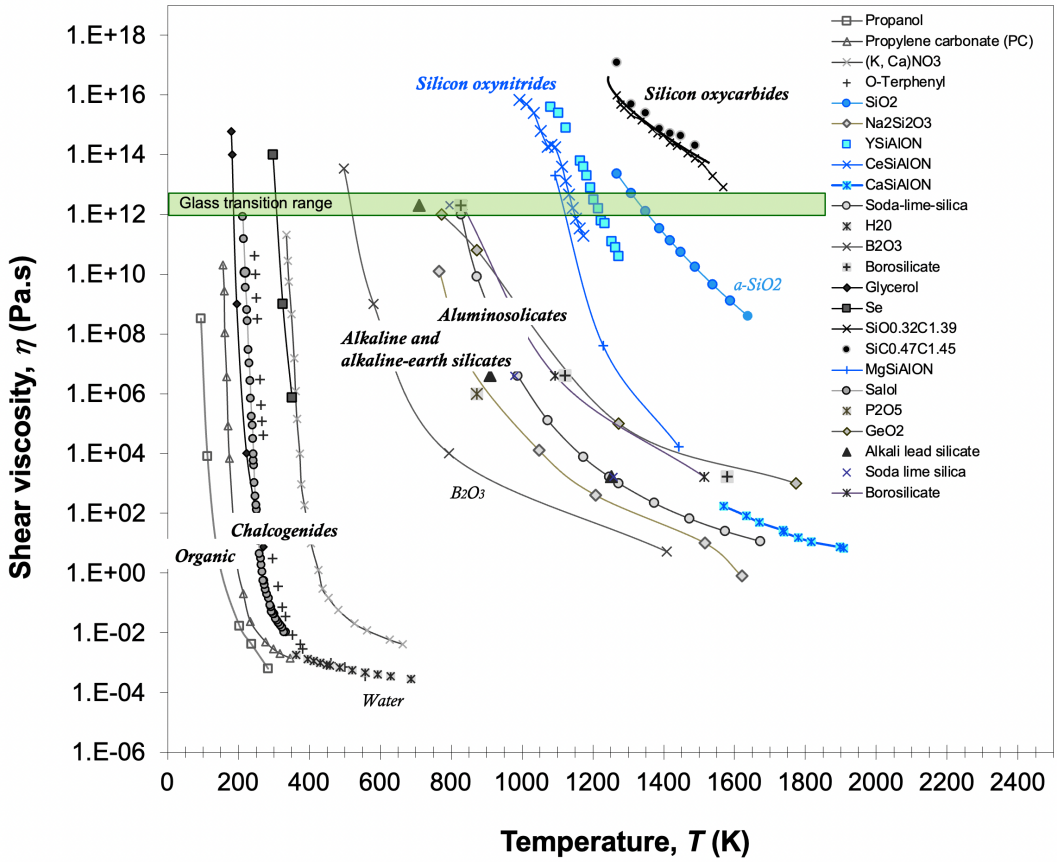

FIGURE 19 Shear viscosity coefficient, η, of glasses from different chemical system.

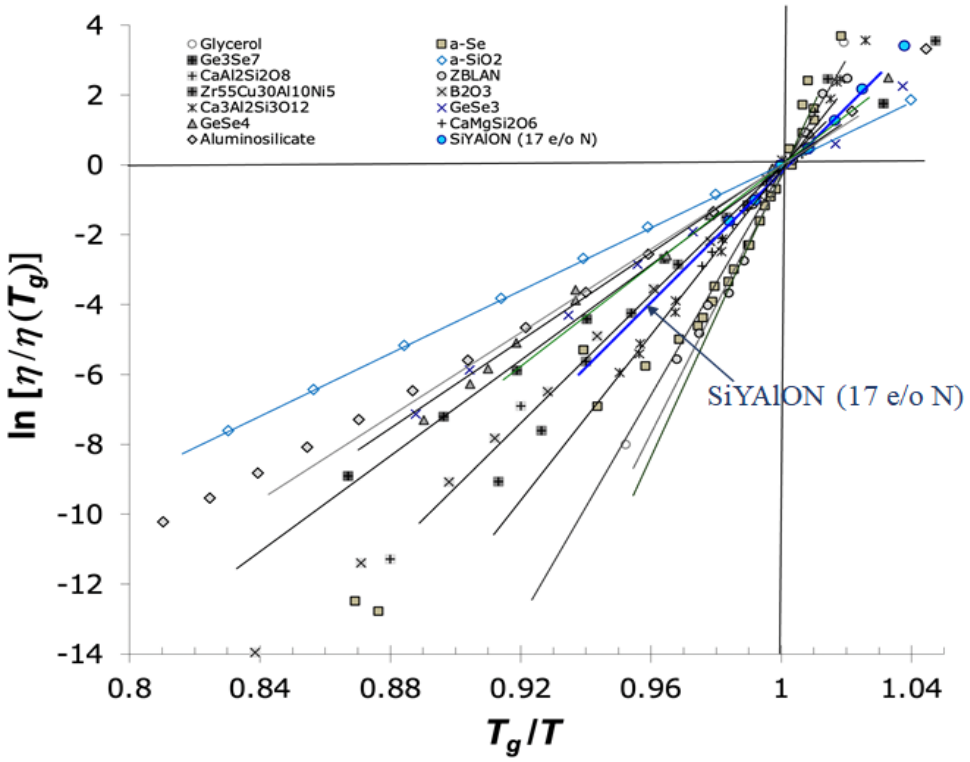

FIGURE 20 T_g-scaled logarithm of the shear viscosity coefficient (η) in the transition range from which the activation energy for flow as well as the fragility index are straightforwardly derived from the slope of the linear intercepts (reprinted and adapted from ref. [199]).

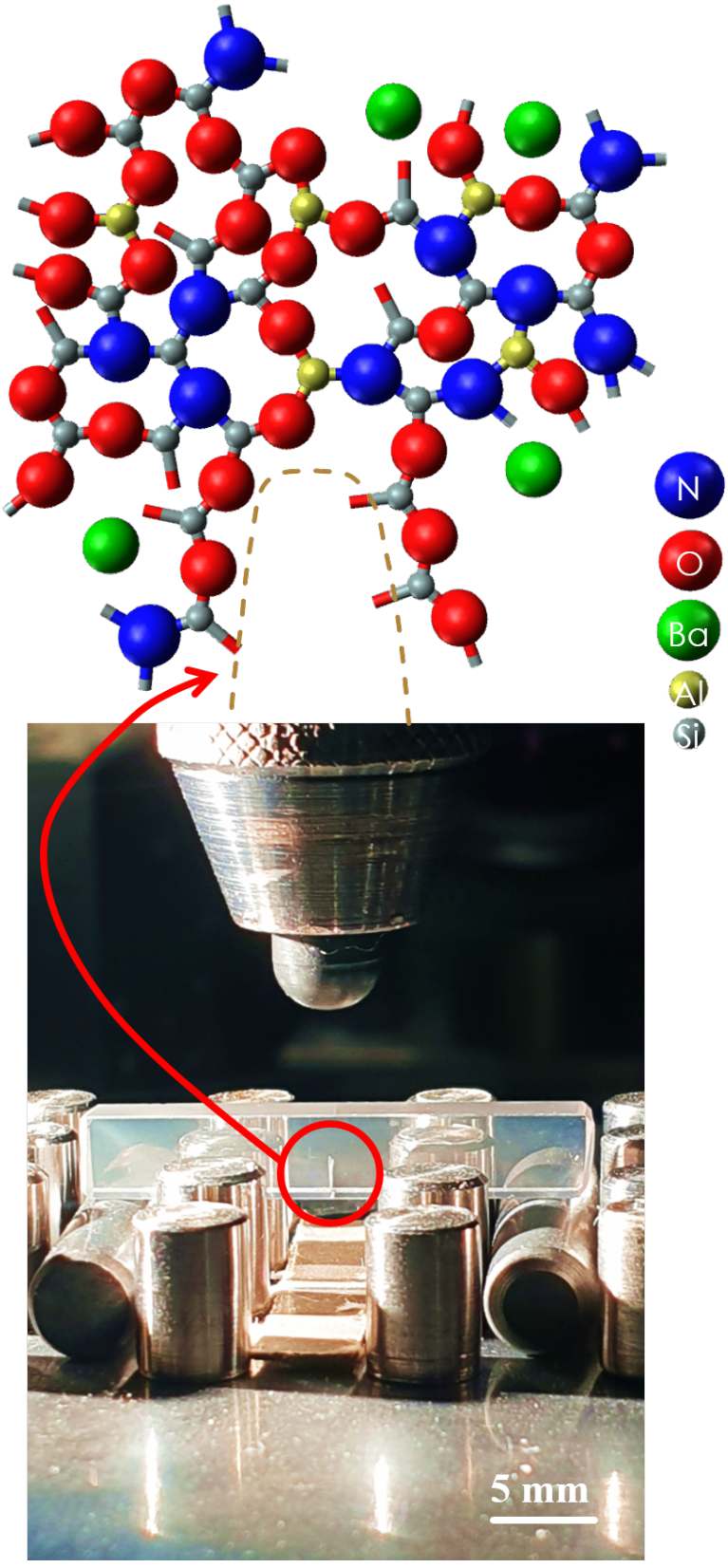

Additional figure (COVER) – $Ba_{0.135}Si_{0.231}Al_{0.02}O_{0.589}N_{0.025}$ pre-cracked parallelepipedic bar for the measurement of K_{Ic} by means of the SEPB method, and schematic drawing of the atomic structure at the vicinity of a crack front.